NATIONAL ADVISORY COMMITTEE FOR AERONAUTICS

TECHNICAL NOTE 3431

AN ANALYSIS OF THE STABILITY AND ULTIMATE COMPRESSIVE STRENGTH OF SHORT SHEET-STRINGER PANELS WITH SPECIAL REFERENCE TO THE INFLUENCE OF RIVETED CONNECTION BETWEEN SHEET AND STRINGER

By Joseph W. Semonian and James P. Peterson

Langley Aeronautical Laboratory
Langley Field, Va.

Washington
March 1955

NATIONAL ADVISORY COMMITTEE FOR AERONAUTICS

TECHNICAL NOTE 3431

AN ANALYSIS OF THE STABILITY AND ULTIMATE COMPRESSIVE STRENGTH OF SHORT SHEET-STRINGER PANELS WITH SPECIAL REFERENCE TO THE INFLUENCE OF RIVETED CONNECTION BETWEEN SHEET AND STRINGER

By Joseph W. Semonian and James P. Peterson

SUMMARY

A method of strength analysis of short sheet-stringer panels subjected to compression is presented which takes into account the effect that the riveted attachments between the plate and the stiffeners have on the strength of panels. An analysis of experimental data shows that panel strength is highly influenced by rivet pitch, diameter, and location and that the degree of influence for a given riveting depends on the panel configuration and panel material.

INTRODUCTION

Rivets have been used extensively for attaching the cover skin to the stringers and webs of aircraft wings. These rivets have been designed, to a large extent, by rule-of-thumb methods; yet, extensive experimental work of which reference 1 is representative has shown that the compressive strength of stiffened panels is greatly influenced by variations in diameter and pitch of the rivets. References 2 to 4, in which the mode of instability of plates in compression known as wrinkling or forced crippling has been analyzed, show that the panel strength is influenced also by the location (rivet offset) as well as the pitch and diameter of the rivets. This mode of instability results from the existence of a flexible attachment between the plate and its supporting members and has occurred more frequently as the compression skins have become heavier and the supporting members lighter.

The purpose of the present paper is to evaluate the strength of short compression panels and in particular to determine the influence of the riveting used to fasten the stringers to the plate on the strength of the

panel. Figure 1 shows the variation in strength with rivet pitch and names the various modes of failure involved. Only rivet pitch is considered to be varied in figure 1 but variations in strength could be obtained also by varying the rivet diameter or the rivet offset. When the rivet pitch is small, the panel of figure 1 fails in the local mode; for larger pitches, it may fail in either the wrinkling or the interrivet mode. Failures in the interrivet mode are not usually permitted in contemporary design; whereas, failures in the wrinkling mode are common. The problem of evaluating the effect of riveting on the strength of panels becomes, therefore, primarily a study of the wrinkling mode of failure. The local-mode section of the curve of figure 1 is shown as a horizontal line. It is recognized that there may be some gain in strength with a favorable change in riveting after the riveting (pitch in fig. 1) is such that the local mode is obtained. The available test data indicate that the gain in strength is small and it is neglected in the analysis presented herein.

A study of the wrinkling mode is made with the use of the procedures established in references 3 and 4 in connection with the calculation of the strength of multiweb beams in bending. These procedures make use of a new structural parameter termed the "effective rivet offset" which plays an important role in determining the strength of riveted structures such as compression panels and multiweb beams and makes possible relatively simple structural analysis. The effective rivet offset is evaluated by using a relatively rigorous analysis of the initial instability of compression panels supplemented by experimental data and is applicable to the analysis of multiweb beams as well as panels. A semiempirical maximum-strength analysis of panels which utilizes the effective-rivet-offset concept is made and compared with a large number of test results to show the accuracy and generality of the analysis. The analysis is exemplified in the appendix.

SYMBOLS

b_A width of attachment flange of stiffener (see fig. 2), in.

b_F width of outstanding flange of stiffener (see fig. 2), in.

b_H width of top of hat for hat-section stiffeners, in.

b_O geometric rivet offset (see fig. 2), in.

b_S stiffener spacing (see fig. 2), in.

b_W depth of web of stiffener (see fig. 2), in.

d rivet diameter, in.

f effective rivet offset (see fig. 5), in.

k_{cr} buckling-stress coefficient

k_M failing-stress coefficient

p rivet pitch, in.

p_a allowable rivet pitch, in.

r_A radius of bend between attachment flange and web of stiffener (see fig. 2), in.

t_S plate thickness (see fig. 2), in.

t_W stiffener thickness (see fig. 2), in.

A_Z cross-sectional area of Z-section stiffener, $in.^2$

D_S plate flexural stiffness per unit width, $E_S t_S^3 / 12(1 - \mu^2)$, kips/in.

D_W flexural stiffness per unit width of web, $E_W t_W^3 / 12(1 - \mu^2)$, kips/in.

E Young's modulus, ksi

E_{sec} secant modulus, ksi

E_{tan} tangent modulus, ksi

E_S Young's modulus of plate material, ksi

E_W Young's modulus of stiffener material, ksi

R rivet tensile strength, kips

R_R required rivet tensile strength, kips

α rotational stiffness per unit length (see fig. 5), kips

$\beta = \dfrac{b_W/t_W}{b_S/t_S}$

δ lateral deflection of plate, in.

η plasticity factor

$\theta = \dfrac{\pi}{\lambda/b_S}\sqrt{\dfrac{\lambda}{b_S}\sqrt{k_{cr}} + 1}$

λ buckle length, in.

μ Poisson's ratio

σ_{cr} buckling stress, ksi

$\bar{\sigma}_f$ average stress in panel at failure, ksi

$\bar{\sigma}_{f_{crip}}$ average stress in panel at failure in local mode, ksi

σ_M failing stress of plate, ksi

$\sigma_{Z_{crip}}$ crippling strength of Z-section stiffener, ksi

$\phi = \dfrac{\pi}{\lambda/b_S}\sqrt{\dfrac{\lambda}{b_S}\sqrt{k_{cr}} - 1}$

ψ deflectional stiffness per unit length, ksi

The designation for the various aluminum alloys has recently been changed. The old designation and the corresponding new designation for the aluminum alloys mentioned in this paper are as follows:

Old designation	New designation
24S-T3	2024-T3
75S-T6	7075-T6
A17S-T3	2117-T3
2S-F	1100-F

STRUCTURAL ANALYSIS

A panel typical of those analyzed is shown in figure 2. The panel is considered to be short enough so that the column bending mode can be neglected yet long enough so that various local modes can form freely without end effects. The panel is considered to be wide with many equally spaced stringers but the results of the analysis can be applied to panels with as few as four stringers without appreciable error.

The analysis is presented in four sections. The first section develops an initial-instability analysis which together with available experimental data is used in the second section to establish the effective rivet offset as a function of appropriate panel parameters. The values of effective rivet offset thus established are used in the third section to formulate a semiempirical maximum-strength analysis. Finally, the fourth section is devoted to developing criteria which limit the pitch and diameter of rivets required to achieve the predicted strength of panels.

Initial Instability of Panels

The panel shown in figure 2 usually will buckle into either the local mode which has been analyzed in reference 5 or the wrinkling mode which will be analyzed herein. Another mode termed the "torsional cum local" mode was analyzed in reference 6. This mode may become the predominant mode when the width of the outstanding flange of the stiffener becomes small $\left(\text{say } b_F < 0.4b_W\right)$ so the flange does not have enough stiffness to prevent the line of intersection between the flange and the web of the stiffener from translating when the panel buckles.

The wrinkling mode of instability can be analyzed by considering the plate to be supported by elastic springs with a deflectional stiffness per unit length of panel ψ as indicated in figure 3. A cross-section of the plate through an up-buckle is shown in figure 4. The stability criterion for the plate is given in reference 3 as

$$\frac{\psi b_S^3}{\pi^4 D_S} = \frac{\dfrac{4\sqrt{k_{cr}}}{\pi^2 \dfrac{\lambda}{b_S}}}{\dfrac{\dfrac{\sin \phi}{\phi}}{1 - \cos \phi} - \dfrac{\dfrac{\sinh \theta}{\theta}}{1 - \cosh \theta}} \tag{1}$$

This expression has been solved and values of k_{cr} are plotted against values of λ/b_s for various values of the parameter $\psi b_s^3/\pi^4 D_s$ in figure 7 of reference 3.

The deflectional stiffness provided by a stringer of the same material as the plate is given by reference 4 as

$$\frac{\psi b_s^3}{\pi^4 D_s} = \frac{\frac{12}{\pi^4}\left(\frac{f}{b_w}\frac{\alpha}{\frac{D_w}{b_w}} + 1\right)}{\left(\frac{f}{b_w}\beta\right)^3\left(\frac{f}{b_w}\frac{\alpha}{\frac{D_w}{b_w}} + 4\right)} \tag{2}$$

where the rotational stiffness α is a function of the web stress and the buckle length and can be taken from reference 7 which uses the symbol $4s^{II}$ to define this stiffness. The assumptions implied in the use of the above formulas have been given in reference 4 but are reviewed here for completeness of the present paper.

Besides the restrictions on length and width of panel as discussed earlier, the implied assumptions are: (1) Deflections are small, (2) the structure is elastic, and (3) the stringer stiffness can be obtained from the idealization shown in figure 5. This idealization is based on the assumptions: (a) The effective rivet offset can be defined as the distance from the web of the stringer to a longitudinal line along which the rivets effectively clamp the attachment flange to the plate, (b) the longitudinal bending stiffness of the attachment flange can be neglected, and (c) the web can be assumed to be simply supported at the bottom. This last assumption will be good as long as the width of the outstanding leg of the Z is about $0.4b_w$. At much larger values, it can become the unstable element and thereby initiate buckling; at much smaller values, it will not have enough depthwise stiffness to provide simple support to the web.

Equations (1) and (2) have been solved and the results are given in figure 6. The buckling coefficient k_{cr} is plotted against the parameter β for various values of the parameter f/b_w. The buckling coefficient is related to the buckling stress by the relation

$$\frac{\sigma_{cr}}{\eta} = k_{cr}\frac{\pi^2 D_s}{b_s^2 t_s} \tag{3}$$

A value of the plasticity factor η that has been found to give good correlation between test and calculation is

$$\eta = \frac{E_{sec}}{E}\left(\frac{1}{2} + \frac{1}{2}\sqrt{\frac{1}{4} + \frac{3}{4}\frac{E_{tan}}{E_{sec}}}\right) \tag{4}$$

This value of η is the value given by Stowell (ref. 8) for long simply supported flat plates in compression.

Local-buckling curves from reference 5 for $b_F/b_W = 0.4$ and $t_W/t_S = 0.63$ and 1.00 have been plotted in figure 6 for comparison with the wrinkling curves.

It will be noted that the buckling coefficient k_{cr} for the wrinkling mode is determined by the two parameters f/b_W and β even though these parameters are not sufficient to determine the panel configuration. The local-buckling curves, for instance, require the additional parameter t_W/t_S to fix their location on the plot of k_{cr} against β. This phenomenon was pointed out in reference 4 in connection with the calculation of wrinkling coefficients for multiweb beams and can be verified experimentally for panels by using data from reference 9. For example, figure 7 shows the failing stress for panels on which all structural parameters were held constant except t_W/t_S and it can be seen that the failing stress is independent of t_W/t_S within the accuracy of the tests. The fact that the data are maximum-strength data rather than buckling data does not appreciably affect the argument because the panels are of such proportions that the failing load is at most a few percent greater than the buckling load and is therefore closely related to the buckling load. The particular values of rivet pitch used in figure 7 were chosen because, after a preliminary study of the data, they were felt to be large enough so that the panels did not fail in the local mode and small enough so that the panels did not fail in the interrivet mode. (See fig. 1.) Other values of rivet pitch and t_W/t_S given in reference 9 further substantiate the insensitiveness of the wrinkling stress to changes in t_W/t_S.

Experimental Determination of f

The analysis developed in the preceding section gives the wrinkling stress of a panel provided the dimension f is known. Conversely, if the wrinkling stress of a panel is known, the value of f can be determined. The existing panel data, however, are not very suitable for determining the dimension f for three main reasons: (1) The rivet offset b_O was usually not varied or even controlled because its influence on panel strength has only recently been understood; (2) the buckling stress was

often never published or perhaps even measured because the interest was mainly directed toward finding the maximum strength of panels; and (3) the cases in which the panels did wrinkle and the buckling load was recorded often involved failure at such high stresses that the effects of plasticity must be known to a high degree of accuracy in order to determine f. In order to alleviate this situation, a series of 7075-T6 (previously designated as 75S-T6) aluminum-alloy panels on which the rivet pitch, diameter, and offset as well as the radius of bend between the attachment flange and the web of the stiffener were systematically varied were built and tested. The results of these tests are reported in table I. These data, and all other available data which were believed to be applicable, were plotted and cross-plotted until a best fit to the data was obtained. The result is shown in figure 8 where the distance f is given in terms of the rivet offset b_0 and the pitch and diameter of the rivets. It will be noted that the radius of bend between the attachment flange and the web of the stringer as well as the type of rivets does not appear on this plot. Furthermore, the other dimensions appear only in very simple form. In spite of this simplicity, it is believed that figure 8 has rather general applicability. For instance, figure 8 can evidently be applied to panels with various types of rivets although most of the data used to establish the figure were obtained from tests on panels on which NACA countersunk rivets were used. The countersunk head of this type of rivet is formed from the rivet shank by driving the rivet and the excess material is then milled off flush. Figure 2 of reference 10 gives a comparison of failing loads for panels assembled with NACA rivets and similar panels assembled with flat-head rivets with the manufacturer's head on the plate side. The comparison shows little or no effect of type of rivet on the strength of panels which obviously failed by wrinkling. A few available tests from panels and multiweb beams which were assembled with universal-head or flat-head rivets on the stiffener side and a shop-driven head on the plate side further indicate that the error in using figure 8 for other types of rivets is small.

The data used to establish the chart of figure 8 were obtained from tests on panels assembled with rivets whose diameter was at least as great as 90 percent of the plate thickness $\left(d/t_s > 0.90\right)$ and the chart should not be used for much smaller values of rivet diameter without confirmation.

Figure 8 is applicable to multiweb beams as well as panels and can be used in the application of the formulas and design charts of reference 4 to the analysis of the bending strength of multiweb beams.

Failure of Panels

The failure of short compression panels usually results from a growth of either local or wrinkling type of buckles. Less frequently, failure

may result from rivet failure or growth of an interrivet type of buckle. The first two types of failures will be discussed in this section and the last two types will be considered in the next section where rivet criteria are developed that can be used to prevent such failures.

Failure in the wrinkling mode.- Panels which buckle initially in the wrinkling mode usually fail in a similar mode. The plate configuration at failure, however, is simpler than the initial buckling configuration because, as the initial buckles grow with an increase in applied load, the plate buckle shape becomes more and more cylindrical until at failure it may be assumed to be cylindrical and the plate may be treated as a column on an elastic foundation. The plate in the column mode appears much like the well-known interrivet mode except the length of buckle is greater than the rivet pitch. The stringer, however, has a very different configuration. In the interrivet mode the stringer cross section may remain essentially undistorted while the plate and stringer separate. In the wrinkling mode of failure the attachment flange of the stringer follows the plate contour and causes the other plate elements of the stringer to distort also. The similarity between the appearances of the wrinkling mode and the interrivet mode has caused investigators to make strength calculations with interrivet-type formulas on panels which failed in the wrinkling mode. (See, for instance, ref. 11.) The panels of this reference evidently failed in the wrinkling mode and the strength of the panels can be calculated by the methods developed herein.

The stability criterion for the plate in the wrinkling mode of failure is given as (see ref. 12)

$$k_M = \frac{1}{\left(\frac{\lambda}{b_S}\right)^2} + \frac{\psi b_S^3}{\pi^4 D_S}\left(\frac{\lambda}{b_S}\right)^2 \tag{5}$$

The support stiffness was determined by trial to give the best correlation between panel strength and calculated strength. It was found that the support stiffness could be taken as

$$\frac{\psi b_S^3}{\pi^4 D_S} = \frac{\frac{12}{\pi^4}\left(3\,\frac{f}{b_W} + 1\right)}{\left(\frac{f}{b_W}\beta\right)^3\left(3\,\frac{f}{b_W} + 4\right)} \tag{6}$$

This equation is identical to equation (2) except the rotational stiffness $\alpha \frac{b_W}{D_W}$ has been replaced by a constant value of 3. In the trial

calculations used to determine the support stiffness, other values of $\alpha \frac{b_w}{D_w}$ were tried, including the apparent value as given by equation (2), but the value $\alpha \frac{b_w}{D_w} = 3$ was considered to give the best agreement between calculated strength and panel strength over a wide range of panel proportions. It gave particularly superior correlation compared with the apparent value when the webs of the stiffeners were relatively unstable because the apparent value (eq. (2)) gave the restraint at the onset of buckling of the webs and not the restraint offered the skin at panel failure. The value $\alpha \frac{b_w}{D_w} = 3$ was also used in reference 4 to calculate the strength of multiweb beams in bending.

With the simplification implied by equation (6), that the support stiffness is independent of the buckle length, equation (5) can be simplified to read

$$k_M = 2\sqrt{\frac{\psi b_s^3}{\pi^4 D_s}} \tag{7}$$

after k_M is minimized with respect to buckle length.

Equations (6) and (7) have been solved and the results are presented in figure 9 which gives the maximum stress that the plate can carry in the wrinkling mode. At this stress, the lateral deflections of the plate, and therefore the lateral forces on the stringers, become large and destroy the capacity of the stringers to carry additional load except for unusual panel proportions.

Experience in testing panels and multiweb beams indicates that a plate in the wrinkling mode suffers a relatively moderate redistribution of stress after initial buckling. The load-shortening curve for a plate in the wrinkling mode, therefore, nearly coincides with the stress-strain curve of the plate material until just prior to plate failure. The stringer on a panel which has buckled in the wrinkling mode appears very much like a stringer on a panel which has buckled in the local mode and evidently suffers much the same redistribution of stress and loss of axial stiffness. In order to calculate the strength of a panel, it is necessary to know the load carried by the stringers at panel failure. (The plate load is given by fig. 9.) The load carried by the stringers depends on the proportions of the panel. If the stringers are relatively sturdy ($\beta < 1$), they will be stressed the same as the plate. If the stringers

are unstable ($\beta > 1$), the stringers will not be loaded as heavily as the plate. An approximation which gives predictions which are slightly high when the stringers are unstable but which gives satisfactory results over the entire practical range of panel proportions is that the stringers take the same stress as the plate as long as that stress is not greater than the stringer crippling stress, in which case the stringers take their crippling stress. In addition, the calculated load carried by the panel must always be greater than the crippling load of the stringers tested without being fastened to the plate. This criterion takes care of the case when the area of the stringers is large compared with the area of the plate and the attachment between the plate and the stringer is so flexible that wrinkling occurs at a load less than the crippling load of the stringers. For this case, the lateral forces on the stringers are comparatively small and do not affect the strength of the stringers. Furthermore, at the shortening necessary for the stringers to achieve their crippling stress, the load being carried by the plate has fallen to a negligible quantity and it may be assumed that the entire load is being carried by the stringers.

The value of the plasticity factor η to be used with figure 9 is given by equation (4). The use of a plasticity factor which is a function only of the stress-strain curve of the plate material and is applied to the average stress in the plate at failure may seem to be rather arbitrary for panels on which the proportions are such that the panels buckle at loads that are considerably less than the loads that the panels ultimately carry. Panels which buckle in the local mode, for instance, experience a severe redistribution of stress as the panel is loaded beyond the buckling load. The factor may not be too arbitrary for panels which fail in the wrinkling mode, however, because a plate in the wrinkling mode of failure is under relatively uniform stress across the width of the plate; that is, the stress is not peaked at the stringers as for a plate which has buckled in the local mode. The correlation between test and calculation obtained by using the plasticity factor given by equation (4) will be given later and indicates that the factor is satisfactory even for panels with a large post-buckling strength.

When figure 9 is used to calculate the strength of a panel, the strength in the local mode as well as the strength in the wrinkling mode should be calculated and the load the panel can be expected to carry will be the lower of the two loads. The strength of panels in the local mode will be discussed in the next section.

Failure in the local mode.- Panels which buckle initially in the local mode may fail as a result of the growth of the local buckles. (See fig. 1.) A few panels have been observed to buckle in the local mode and to switch from local buckling to wrinkling at a higher stress level and eventually fail in the wrinkling mode. The data from such panels evidently would plot near the value of rivet pitch in figure 1 where the local mode ends and the wrinkling mode starts.

A study of the available data on compression panels on which the pitch and diameter of the attachment rivets were varied indicates that the gain in strength corresponding to a decrease in pitch or an increase in diameter of the rivets after the local buckling range has been reached is small. Consequently, for riveted panels there is a panel strength which is relatively independent of changes in riveting that corresponds to failure of the panel in the local mode. This characteristic has been recognized for a long time (see, for instance, ref. 10) and is responsible for the numerous investigations in the past on "strongly riveted panels" (the investigation of ref. 5, for instance). An obvious question that usually arose when these investigations were applied to the design of panels was that the riveting required to make the panel behave as a strongly riveted panel was not known and rather severe rivet criteria had to be used. (See criterion of ref. 13.) The present analysis alleviates this difficulty for panels by relating the strength of panels to the pitch, diameter, and offset of the attachment rivets.

Reference 5 shows that the ultimate strength of panels which buckle locally at high stresses is closely related to the buckling load and can be calculated by the buckling charts of that reference. The particular curves for a value of $\frac{b_F}{b_W}$ of 0.4 and values of $\frac{t_W}{t_S}$ of 0.63 and 1.00 are reproduced in figure 6. Reference 14 gives a method of predicting the strength of a panel in the local mode provided the strength of a nominally identical panel of another material is known. With the help of these references and the test data of references 1, 9, and 15 to 19, the strength of some panels which fail in the local mode was estimated and is given in figure 10. In the construction of figure 10, the method of reference 5 determined the indicated strength of the panels when the failing stress is high (usually panels with values of β of about unity and with small values of b_S/t_S and b_W/t_W). These particular panels require the most severe riveting criteria in order to force the panel to fail in the local mode and consequently their strengths are the most difficult to obtain experimentally. The available experimental data, supplemented by the procedure of reference 14, sufficed to determine the strengths of the other panels considered.

Rivet Criteria

The maximum-strength analysis of compression panels given in the preceding section requires certain limitations on the pitch and strength of rivets in order that the panel will carry the predicted load. The rivets must be spaced closely enough and have adequate strength to make the stringer flange follow the plate contour. If the spacing is too large, the panel may fail by interrivet buckling. If the strength is insufficient, the panel may fail prematurely because of rivet failure.

Rivet pitch.- An expression for buckle length which is consistent with the maximum-strength formulas (6) and (7) is

$$\frac{\lambda}{b_S} = \sqrt{\frac{2}{k_M}} \tag{8}$$

The allowable rivet pitch which must not be exceeded in order that the stringer flange follow the plate contour can logically be related to the buckle length as given by equation (8). It was found by trial that, if the rivet pitch was less than 90 percent of the calculated buckle length, wrinkling would occur rather than interrivet buckling. Hence, the rivet pitch must satisfy the criterion

$$\frac{p}{b_S} < 0.90\sqrt{\frac{2}{k_M}} \tag{9}$$

Rivet strength.- The lateral force required to hold the compressed plate in its deflected position is proportional to the support stiffness and the lateral deflection of the plate. The force on a rivet near the crest of a buckle may be expressed approximately as

$$R \approx \psi \delta p \tag{10}$$

where δ is the lateral deflection of the plate at the crest of a buckle. The value of ψ may be taken from equation (A19) of reference 4. An appropriate value for the rotational stiffness $\frac{\alpha f}{D_f}$ in this equation is $\frac{\alpha f}{D_f} = 3\frac{f}{b_W}$. In order to express equation (10) as a rivet-strength criterion, the value of lateral deflection must be known or assumed. Figure 3 of reference 20 indicates that, for an idealized H-section column, maximum load is reached before the lateral deflection is one-fifth of the column (or plate) thickness provided the buckling stress is at least half of the compressive yield stress of the column material. If this value is used in formula (10), the required tensile strength for a rivet becomes

$$R_R > \frac{E_W}{1-\mu^2}\frac{1}{\left(\frac{f}{t_W}\right)^3}\left(\frac{3\frac{f}{t_W}+\frac{b_W}{t_W}}{3\frac{f}{t_W}+4\frac{b_W}{t_W}}\right)\frac{t_S}{5}p \tag{11}$$

The tensile strength of a rivet is defined as the load required to cause any failure; it may be the load required to break the shank but more often it is the load required to pull the countersunk head through the plate or, when the stiffener gage is small, to pull the rivet head through the stiffener.

Reference 21 gives the strength of protruding-head rivets. Reference 22 gives strength data on NACA countersunk and conventional countersunk rivets. Additional rivet-strength data can be found in references 23 and 13.

Expression (11) gives the tensile strength of the attachment rivets that is required in order that the predicted strength of the panel in the wrinkling mode can be achieved. Obviously, when the panel fails in the local mode, expression (11) does not apply. The available data indicate that for this case the rivet strength need not be any greater than that required when failure is in the wrinkling mode and the stress levels at failure in the two modes are equal.

EXPERIMENTAL VERIFICATION

The data presented in this section have already been used to establish the empirical factors in the analysis presented earlier and will now be compared with the analysis to assess its validity. The data were taken, in large part, from published NACA panel data obtained from panels which were five bays wide (6 stringers) and had a slenderness ratio L/ρ of 20. The ends of the panels were ground flat and parallel in a special grinder prior to testing and the panels were tested flat-ended in a hydraulic testing machine. A large amount of wrinkling data is available on panels made from 2024-T3 (previously designated 24S-T3) aluminum alloy. The number of tests on panels which failed in the wrinkling mode and which were made from 7075-T6 aluminum alloy is much smaller for two reasons: (1) The investigation on the effect of riveting on panel strength was made on 2024-T3 aluminum-alloy panels first and later on 7075-T6 aluminum-alloy panels. The knowledge gained from the early experiments could be applied to the later tests and thereby reduce the number of tests required. (2) The tests on 7075-T6 aluminum-alloy panels were made on panels with extruded stringers with small fillets so the rivet line could be moved in close to the web of the stiffener and thereby prevent the wrinkling type of failure. In order to relieve the shortage of data on 7075-T6 aluminum-alloy panels, a series of panel tests were made in the present investigation and are reported herein.

Data on panels with riveting which do not satisfy the criteria of expressions (9) and (11) and the additional criterion that the ratio p/d

must be less than 15 will not be given in the presentation which follows. The latter criterion is included because available data on panels for which the failure was definitely wrinkling were considered to be inadequate to establish design curves for these high values of p/d. The restriction on panel design imposed by this criterion, however, is not considered to be severe because contemporary design rarely allows such large rivet pitches.

2024-T3 Aluminum-Alloy Panels

The data of references 9, 15, and 16 are shown in figures 11, 12, and 13, respectively, where the average stress in the panel at failure $\bar{\sigma}_f$ is plotted against the rivet parameter p/d. The data of reference 15 for panels with a b_s/t_s greater than 50 are not given because it is relatively easy to rivet such panels so that the panel will fail in the local mode. NACA countersunk rivets were used to assemble the panels. Other pertinent dimensions are given in the figures. The data plot against the parameter p/d with a small amount of scatter. This characteristic is responsible for the use of the $\frac{p}{d}$- parameter on the f-chart of figure 8.

The curves in figures 11 to 13 represent predicted panel strengths. The wrinkling section of the curves was obtained with the use of figures 8 and 9. For the panels represented by the data in figure 13, where the stringers are relatively unstable, the crippling strength of the stringers was required to obtain the panel strength in the wrinkling mode. The stringer crippling strength was taken from reference 24; the data were extrapolated when it was necessary. The curves predict the trend as well as the magnitude of the data within the accuracy of the panel tests; experience in testing panels indicates that strength tests on two nominally identical panels usually give strengths which differ by less than 5 percent from the average strength although differences as great as 10 percent have been obtained. The wrinkling curves miss the middle of the scatter band of the data in some instances by about 5 percent. It is believed that such discrepancies are largely a result of neglecting the difference in material properties and panel parameters (particularly b_o/t_w) between one group of panels and another. The panels represented by the data of figures 12 and 13 were built in groups similar to the grouping used in the presentation of the data and are therefore particularly susceptible to errors common to a group of data. These differences were neglected in the presentation of the data because of the resulting simplicity and because only nominal values of the rivet offset b_o were known.

The local-mode section of the curves in figures 11 to 13 were obtained from figure 10 for the panel proportions covered by the figure. The local strength of the panels with a b_w/t_w of 25 and 50 which are not covered by figure 10 were obtained by interpolation and extrapolation of the data from figure 10 by using the present data as a guide. A study of figures 11 to 13 indicates that the strength of a panel in the local mode becomes increasingly difficult to attain as t_w/t_s is increased or as b_s/t_s is decreased. Accordingly, the closest riveting used in the investigation ($p/d = 3.0$) was just adequate to attain the strength in the local mode of the panels of figure 11 with a thickness ratio $t_w/t_s = 1.00$ and was inadequate to attain the local strength of the panels with $t_w/t_s = 1.25$. For panels with much smaller values of b_s/t_s than were used in figure 11, it would be impossible to rivet the panels so that the local strength is obtained without the use of smaller values of the rivet offset b_o.

Some test data from reference 25 on panels with hat-section stiffeners is given in figure 14. The average stress in the panel at failure $\bar{\sigma}_f$ is plotted against b_s/t_s where $2b_s$ is the distance between similar locations on two adjacent hat stiffeners. Only data for the thickness ratio $t_w/t_s = 0.39$ are shown because they are considered to be sufficient to establish the concept that for panels with unequal stiffener spacings an average spacing can be used for predicting the maximum load of the panel in the wrinkling mode of failure. The particular thickness ratio $t_w/t_s = 0.39$ was chosen rather than some other because the panels with other thickness ratios had stiffer attachments between the hat-section stiffeners and the plate so that most of these panels fail in the local mode rather than in the wrinkling mode. The data for panels with elements having a width-thickness ratio b/t greater than 50 have not been shown.

The calculated curves in figure 14 are based on an average measured value of b_o/t_w rather than the nominal value.

7075-T6 Aluminum-Alloy Panels

The data of table I are shown in figure 15 where the average stress in the panel at failure is plotted against the parameter $\frac{f/t_w}{b_s/t_s}$. The predicted panel strengths are indicated by the curves and agree with the test data within the accuracy of the data. The shaded test points represent panels which had stringers with a value of $\frac{r_A}{t_w}$ of 6. Since

the stringers had a value of $\frac{b_W}{t_W}$ of 20, these stringers had a value of $\frac{r_A}{b_W}$ of 0.30. These points all appear high on the figure and indicate that the attachment between the stringer and the plate was actually stiffer than figure 8 indicates. It is not known whether the test loads were high because r_A/t_W was large or whether it was because r_A/b_W was large or both. Inasmuch as the chart gives conservative predictions in this range, the uncertainty is not serious.

DISCUSSION OF RESULTS

A method has been developed whereby the strength of panels is related to the design of the attachment between the plate and the stiffener. The method makes use of an experimentally determined effective rivet offset f which is an important dimension in the determination of the strength of panels. The importance of this dimension as well as other panel dimensions on the strength of panels can be readily seen from the equation

$$\frac{\sigma_M}{\eta} = \frac{E}{1-\mu^2}\sqrt{\frac{1}{3}\,\frac{1}{\frac{b_S}{t_S}}\,\frac{1}{\left(\frac{f}{t_W}\right)^3}\,\frac{3\,\frac{f}{t_W}+\frac{b_W}{t_W}}{3\,\frac{f}{t_W}+4\,\frac{b_W}{t_W}}} \tag{12}$$

This equation gives the strength of a plate in the wrinkling mode and is equivalent to the chart of figure 9. It is seen that the failing stress of the plate is approximately inversely proportional to $f^{3/2}$. Equation (12) has been used to estimate the strength of compression panels covering a wide range of the structural parameters t_W/t_S, b_S/t_S, and b_W/t_W and was found to give satisfactory correlation with test results.

The f-chart of figure 8 was constructed from data of tests on 2024-T3 and 7075-T6 aluminum-alloy panels and multiweb beams which were assembled with 2117-T3 (previously designated A17S-T3) aluminum-alloy rivets. Since the rivet stiffness is a contributing factor in the determination of the effective rivet offset f, changes in rivet material can be expected to make corresponding changes in f which would show up in a panel test as a change in panel strength. Reference 13, however, indicates that very little increase in panel strength can be expected from the use of rivet materials with a higher modulus of elasticity and strength than those of

2117-T3 aluminum alloy but reports on panels with one rivet material (FS-1 magnesium) which had a smaller modulus of elasticity and strength and which failed at loads that were consistently less than those of the panels with 2117-T3 aluminum-alloy rivets. Similarly, reference 13 reports on panels with blind-type Cherry rivets (AN 463) which failed at loads less than those of the panels with 2117-T3 aluminum-alloy rivets. Figure 8 should be used with caution, therefore, for rivet materials whose modulus of elasticity and strength are less than those of 2117-T3 aluminum alloy when used with aluminum-alloy sheet. The panels of reference 13 that were assembled with 1100-F (previously designated 2S-F) aluminum-alloy rivets do not satisfy the strength criterion of expression (11) and their low strengths are attributed to the low tensile strength of the rivets.

Frequently panels are assembled by using extruded stringers which have a right-angle exterior corner between the web and the attachment flange. The use of such stringers usually eliminates the wrinkling mode except for very unusual proportions for two main reasons: (1) The small fillet between the web and the flange of the stringer allows the rivet to be moved in close to the web so that the rivet offset b_0 is reduced and as a consequence f is also reduced and (2) the deflectional stiffness of such a stringer is greater than that of a bent-up stringer of similar proportions with the same rivet offset because of the large stiffness when the plate buckles toward the stringer. For this case, the stiffness may be more nearly that of the web rather than that of the cantilevered flange because the plate can bear directly on the web. The effective stiffness which determined the rivet offset f is some combination of this stiffness and the stiffness for the case when the plate buckles away from the stringer as shown in reference 4. The number of available tests are insufficient to establish a chart such as figure 8 for extruded stringers. These tests (from refs. 13, 18, and 19) indicate that figure 8 can be used to obtain a conservative estimate of the effective rivet offset. Expressions (9) and (11) for the required pitch and strength of rivets can also be used.

Previous investigations of the effect of riveting on the strength of panels of which reference 13 is the most recent have developed a rivet criterion whereby the strength of a panel with a given riveting (given pitch and diameter) is related to the strength of a similar but strongly riveted panel (panel which reaches its potential strength) by a master curve. The master curve is based on the lower limit of test data from panels of various configurations that were constructed of 2024-T3 and 7075-T6 aluminum alloy and were assembled with rivets of various materials. The present investigation has made a more detailed study of the data for panels with the smaller rivet pitches - the data on panels with p/d greater than 15 as well as the data on panels which developed interrivet buckling have not been analyzed. With this restrictive scope and the help

of recently developed procedures of stress analysis, it was possible to make more accurate correlation of the strength of these panels with the riveting used to assemble the panels. For instance, the present investigation utilizes the concept that, after a certain critical value of f/t_w has been reached by decreasing the rivet pitch and/or offset and/or increasing rivet diameter, little or no additional gain in panel strength can be expected by further changes in rivet pitch, diameter, and offset. This critical value of f/t_w is different for different panel configurations. It is more difficult to achieve when the thickness ratio t_w/t_s is large or when the parameter b_s/t_s is small and in extreme cases may be impossible to achieve in riveted panels. The present investigation also makes use of the fact that variations in panel strength for a given change in riveting can be much greater for 7075-T6 aluminum-alloy panels than for 2024-T3 aluminum-alloy panels because plasticity may play a much smaller part in determining the strength of the 7075-T6 aluminum-alloy panels.

CONCLUSIONS

A method of strength analysis of short compression panels has been presented which relates the panel strength to the pitch, diameter, and location of the rivets used to assemble the panel. A large number of panels have been analyzed with this method. These panels covered a wide range of panel configurations. They had elements with aspect ratios b/t which ranged from 20 to 50 and were assembled with rivets which had pitch-diameter ratios p/d of from 3 to 15. Both 2024-T3 and 7075-T6 aluminum-alloy panels were considered. The following conclusions can be made from these studies:

1. Panel strength is highly influenced by variations in rivet pitch, diameter, and location.

2. Favorable variations in the pitch, diameter, and location of rivets for a given panel results in increased panel strength until the riveting is adequate to force failure in the local mode; further variations in riveting will produce negligible increases in panel strength.

3. The minimum riveting specifications that will force the panel to fail in the local mode depend on the panel configuration and on the panel material.

Langley Aeronautical Laboratory,
National Advisory Committee for Aeronautics,
Langley Field, Va., January 17, 1955.

APPENDIX

NUMERICAL EXAMPLE

The use of the design charts and design procedures set forth in the body of the paper are exemplified by analyzing a short, 2024-T3 aluminum-alloy, Z-stiffened, compression panel which is similar to the one shown in figure 2 and has the following dimensions and structural parameters:

$t_W = 0.064$ in.	$b_W/t_W = 40.0$
$t_S = 0.102$ in.	$b_F/b_W = 0.40$
$t_W/t_S = 0.63$	$b_A/t_W = 8.0$
$b_S/t_S = 30.0$	$b_O/t_W = 5.0$

The panel is assembled with 3/32-inch, brazier-head (AN 456), 2117-T3 aluminum-alloy rivets spaced at 1 inch. The rivets have the manufacturer's head on the plate side and a shop-driven head on the stiffener side. Young's modulus of elasticity E is assumed to be 10,600 ksi and Poisson's ratio μ is taken as 0.32.

Additional parameters and information that can be obtained after the panel proportions are given and which will be useful in the analysis which follows are the parameters β and p/d, the area of a stringer A_Z, and corresponding area of plate $b_S t_S$, the local crippling stress of a stringer $\sigma_{Z_{crip}}$, and the strength of the panel in the local mode $\bar{\sigma}_{f_{crip}}$. These parameters are as follows:

$$\beta = \frac{b_W/t_W}{b_S/t_S} = \frac{40.0}{30.0} = 1.33$$

$$p/d = \frac{1.00}{3/32} = 10.7$$

$$A_Z = t_W^2\left(\frac{b_W}{t_W} + \frac{b_A}{t_W} + \frac{b_F}{b_W}\frac{b_W}{t_W}\right) = (0.064)^2\left[40.0 + 8.0 + 0.40(40.0)\right]$$

$$= 0.262 \text{ in.}^2$$

$$b_S t_S = \frac{b_S}{t_S} t_S^2 = 30.0(0.102)^2 = 0.312 \text{ in.}^2$$

$$\sigma_{Z_{crip}} = 27.5 \text{ ksi (ref. 24)}$$

$$\bar{\sigma}_{f_{crip}} = 31.6 \text{ ksi (fig. 10)}$$

When p/d and b_0/t_W are given, f/t_W can be read from figure 8 as

$$f/t_W = 6.98$$

The value of f/b_W is computed as follows:

$$\frac{f}{b_W} = \frac{f/t_W}{b_W/t_W} = \frac{6.98}{40.0} = 0.175$$

From figure 6,

$$k_{cr} = 2.38 \text{ (wrinkling)}$$

$$k_{cr} = 2.45 \text{ (local buckling, extrapolated)}$$

The panel should wrinkle at (see formula (3))

$$\sigma_{cr}/\eta = 25.5 \text{ ksi}$$

and since the plasticity factor for 2024-T3 aluminum alloy is unity at this stress

$$\sigma_{cr} = 25.5 \text{ ksi}$$

From figure 9

$$k_M = 3.64$$

and σ_M/η is computed as

$$\sigma_M/\eta = 39.2$$

With the use of a curve for σ against σ/η for 2024-T3 aluminum alloy with a compressive yield stress (0.2-percent offset stress) of 43.6 ksi, the plate failing stress is found to be

$$\sigma_M = 34.1 \text{ ksi}$$

Since σ_M is greater than the local crippling stress of the stringer found earlier, the load that the panel will carry in the wrinkling mode is determined by adding the loads carried by the stringers and the plate. The average stress in the panel is the panel load divided by the panel area; that is,

$$\bar{\sigma}_f = \frac{\sigma_M b_S t_S + \sigma_{Z_{crip}} A_Z}{b_S t_S + A_Z} = \frac{34.1(0.312) + 27.5(0.262)}{0.312 + 0.262} = 31.1 \text{ ksi}$$

The stress $\bar{\sigma}_f$ is less than $\bar{\sigma}_{f_{crip}}$ found earlier so the panel should fail by wrinkling provided the criteria on rivet pitch and strength are met. By expression (9), the maximum allowable rivet pitch p_a is given as

$$p_a = 0.90\sqrt{\frac{2}{3.64}}\,(30.0)(0.102) = 2.04 \text{ in.}$$

The actual rivet pitch of 1.00 inch is therefore small enough to prevent interrivet buckling. The allowable rivet strength is (expression (11))

$$R_R = \frac{10{,}600}{\left[1 - (0.32)^2\right]} \frac{1}{(6.98)^3} \left[\frac{3(6.98) + 40}{3(6.98) + 160}\right] \frac{0.102}{5} (1.00) = 0.239 \text{ kips}$$

The load required to break the shank of a 3/32-inch rivet based upon an allowable stress of 57.0 ksi is 0.394 kips. Reference 21 shows that the rivet in question will shear its head at 68 percent of the load required to break the shank; therefore,

$$R = 0.68\ (0.394) = 0.268 \text{ kips}$$

which is adequate rivet strength. The predicted buckling and failing stresses are those given previously.

REFERENCES

1. Dow, Norris F., and Hickman, William A.: Effect of Variation in Rivet Diameter and Pitch on the Average Stress at Maximum Load for 24S-T3 and 75S-T6 Aluminum-Alloy, Flat, Z-Stiffened Panels That Fail by Local Instability. NACA TN 2139, 1950.

2. Bijlaard, P. P., and Johnston, G. S.: Compressive Buckling of Plates Due to Forced Crippling of Stiffeners. Preprint No. 408, S.M.F. Fund Paper, Inst. Aero. Sci., Jan. 1953.

3. Anderson, Roger A., and Semonian, Joseph W.: Charts Relating the Compressive Buckling Stress of Longitudinally Supported Plates to the Effective Deflectional and Rotational Stiffness of the Supports. NACA TN 2987, 1953.

4. Semonian, Joseph W., and Anderson, Roger A.: An Analysis of the Stability and Ultimate Bending Strength of Multiweb Beams With Formed-Channel Webs. NACA TN 3232, 1954.

5. Gallaher, George L., and Boughan, Rolla B.: A Method of Calculating the Compressive Strength of Z-Stiffened Panels That Develop Local Instability. NACA TN 1482, 1947.

6. Argyris, J. H., and Dunne, P. C.: Part 2. Structural Analysis. Structural Principles and Data, Handbook of Aeronautics, No. 1, Pitman Pub. Corp. (New York), 1952.

7. Kroll, W. D.: Tables of Stiffness and Carry-Over Factor for Flat Rectangular Plates Under Compression. NACA WR L-398, 1943. (Formerly NACA ARR 3K27.)

8. Stowell, Elbridge Z.: A Unified Theory of Plastic Buckling of Columns and Plates. NACA Rep. 898, 1948. (Supersedes NACA TN 1556.)

9. Dow, Norris F., and Hickman, William A.: Effect of Variation in Diameter and Pitch of Rivets on Compressive Strength of Panels With Z-Section Stiffeners. I - Panels With Close Stiffener Spacing That Fail by Local Buckling. NACA WR L-44, 1945. (Formerly NACA RB L5G03.)

10. Dow, Norris F., and Hickman, William A.: Preliminary Investigation of the Relation of the Compressive Strength of Sheet-Stiffener Panels to the Diameter of Rivet Used for Attaching Stiffeners to Sheet. NACA WR L-61, 1944. (Formerly NACA RB L4I13.)

11. Holt, Marshall: Results of Edge-Compression Tests on Stiffened Flat-Sheet Panels of Alclad and Nonclad 14S-T6, 24S-T3, and 75S-T6 Aluminum Alloys. NACA TN 3023, 1954.

12. Timoshenko, S.: Theory of Elastic Stability. McGraw-Hill Book Co., Inc., 1936.

13. Dow, Norris F., Hickman, William A., and Rosen, B. Walter: Effect of Variation in Rivet Strength on the Average Stress at Maximum Load for Aluminum-Alloy, Flat, Z-Stiffened Compression Panels That Fail by Local Buckling. NACA TN 2963, 1953.

14. Dow, Norris F., and Anderson, Roger A.: Prediction of Ultimate Strength of Skin-Stringer Panels From Load-Shortening Curves. Preprint No. 431, S.M.F. Fund Preprint, Inst. Aero. Sci., Jan. 1954.

15. Dow, Norris F., and Hickman, William A.: Effect of Variation in Diameter and Pitch of Rivets on Compressive Strength of Panels With Z-Section Stiffeners - Panels of Various Stiffener Spacings That Fail by Local Buckling. NACA TN 1467, 1947.

16. Dow, Norris F., and Hickman, William A.: Effect of Variation in Diameter and Pitch of Rivets on Compressive Strength of Panels With Z-Section Stiffeners - Panels That Fail by Local Buckling and Have Various Values of Width-to-Thickness Ratio for the Webs of the Stiffeners. NACA TN 1737, 1948.

17. Schuette, Evan H.: Charts for the Minimum-Weight Design of 24S-T Aluminum-Alloy Flat Compression Panels With Longitudinal Z-Section Stiffeners. NACA Rep. 827, 1945. (Supersedes NACA WR L-197.)

18. Hickman, William A., and Dow, Norris F.: Data on the Compressive Strength of 75S-T6 Aluminum-Alloy Flat Panels Having Small, Thin, Widely Spaced, Longitudinal Extruded Z-Section Stiffeners. NACA TN 1978, 1949.

19. Hickman, William A., and Dow, Norris F.: Data on the Compressive Strength of 75S-T6 Aluminum-Alloy Flat Panels With Longitudinal Extruded Z-Section Stiffeners. NACA TN 1829, 1949.

20. Wilder, Thomas W., III, Brooks, William A., Jr., and Mathauser, Eldon E.: The Effect of Initial Curvature on the Strength of an Inelastic Column. NACA TN 2872, 1953.

21. Schuette, Evan H., Bartone, Leonard M., and Mandel, Merven W.: Tensile Tests of Round-Head, Flat-Head, and Brazier-Head Rivets. NACA TN 930, 1944.

22. Mandel, Merven W., and Bartone, Leonard M.: Tensile Tests of NACA and Conventional Machine-Countersunk Flush Rivets. NACA WR L-176, 1944. (Formerly NACA ARR L4F06.)

23. Schuette, Evan H., and Niles, Donald E.: Data on Optimum Length, Shear Strength, and Tensile Strength of Age-Hardened 17S-T Machine-Countersunk Rivets in 75S-T Sheet. NACA TN 1205, 1947.

24. Lundquist, Eugene E., Schuette, Evan H., Heimerl, George J., and Roy, J. Albert: Column and Plate Compressive Strengths of Aircraft Structural Materials - 24S-T Aluminum-Alloy Sheet. NACA WR L-190, 1945. (Formerly NACA ARR L5F01.)

25. Hickman, William A., and Dow, Norris F.: Compressive Strength of 24S-T Aluminum-Alloy Flat Panels With Longitudinal Formed Hat-Section Stiffeners Having Four Ratios of Stiffener Thickness to Skin Thickness. NACA TN 1553, 1948.

TABLE I

TEST DATA AND PROPORTIONS OF 7075-T6 ALUMINUM-ALLOY PANELS

$\left[\frac{b_F}{b_W} = 0.40\right]$

t_W, in.	t_W/t_S	L/ρ	b_S/t_S	b_W/t_W	b_O/t_W	r_A/t_W (a)	d, in. (b)	p/d	σ_{cr}, ksi	$\bar{\sigma}_f$, ksi
0.0660	0.640	20	24.6	18.7	5.2	3.0	1/16	14.0	45.2	45.2
.0663	.636	20	24.5	18.5	5.0	3.0	3/32	9.3	49.5	52.0
.0668	.650	20	24.8	19.2	6.2	3.0	3/32	9.3	48.0	48.5
.0663	.630	20	24.3	19.4	7.2	3.0	3/32	9.3	41.0	44.3
.0658	.640	20	24.8	19.6	8.6	3.0	3/32	9.3	38.8	41.2
.0666	.645	20	24.7	18.2	5.0	3.0	1/8	7.0	54.0	55.0
.0660	.628	20	24.2	19.2	6.1	3.0	1/8	7.0	51.3	53.0
.0666	.635	20	24.2	19.2	7.1	3.0	1/8	7.0	45.4	48.1
.0662	.633	20	24.4	19.4	8.3	3.0	1/8	7.0	42.1	45.3
.0664	.641	20	24.6	18.3	5.1	3.0	5/32	5.6	55.4	56.2
.0664	.630	20	24.2	19.4	6.2	3.0	5/32	5.6	53.2	54.6
.0660	.638	20	24.6	19.5	7.4	3.0	5/32	5.6	49.2	51.0
.0664	.633	20	24.3	19.2	8.2	3.0	5/32	5.6	45.8	47.6
.0663	.634	20	24.4	19.0	5.4	3.0	3/16	4.7	58.7	59.2
.0666	.636	20	24.4	19.2	6.1	3.0	3/16	4.7	55.2	57.0
.0666	.636	20	24.4	19.3	7.2	3.0	3/16	4.7	50.3	52.8
.0662	.631	20	24.4	19.4	8.2	3.0	3/16	4.7	46.8	50.2
.0647	.620	20	24.5	18.2	3.8	1.0	5/32	5.6	60.7	62.8
.0663	.640	20	24.5	19.3	6.6	4.0	5/32	5.6	53.1	54.6
.0665	.639	20	24.5	19.3	7.2	5.0	5/32	5.6	49.6	52.0
.0657	.635	20	24.7	19.6	8.5	6.0	5/32	5.6	49.7	51.3
.0663	.641	20	24.6	19.0	8.1	6.0	5/32	5.6	50.5	52.5
.0641	.610	20	24.2	18.5	4.5	1.0	5/32	5.6	59.7	62.0
.0650	.625	20	24.6	18.3	5.5	1.0	5/32	5.6	55.0	56.3
.0643	.610	20	24.2	18.5	6.5	1.0	5/32	5.6	52.5	54.2
.0643	.615	20	24.4	18.4	7.6	1.0	5/32	5.6	48.4	49.8
.0627	.605	30	39.5	19.0	4.1	1.0	5/32	5.6	27.6	46.4
.0658	.639	30	39.6	19.6	5.3	3.0	5/32	5.6	26.5	44.9
.0659	.633	30	39.2	19.5	6.4	4.0	5/32	5.6	24.2	42.7
.0648	.627	30	39.5	19.8	7.3	5.0	5/32	5.6	24.6	43.7
.0658	.630	30	39.0	19.3	8.3	6.0	5/32	5.6	26.2	41.2
.0660	.636	30	39.3	19.4	8.2	6.0	5/32	5.6	25.5	39.2

[a]Stringers with $r_A/t_W = 1.0$ were extruded. All others were formed.

[b]All rivets were 2117-T3 flat-head rivets with NACA countersink on the plate side. The depth of countersink for the 1/16-, 3/32-, 1/8-, 5/32-, and 3/16-inch-diameter rivets was 0.040, 0.050, 0.060, 0.070, and 0.080, respectively.

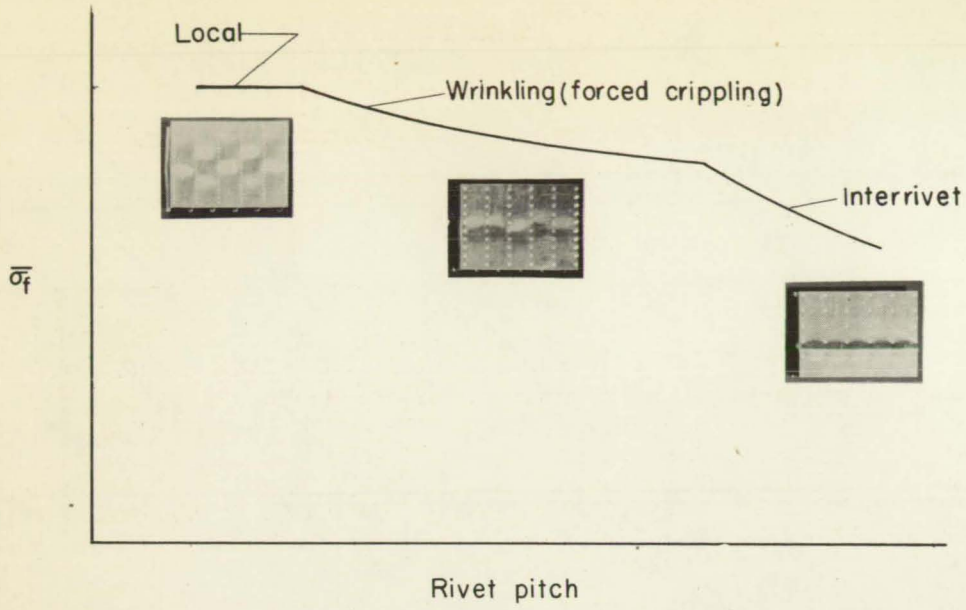

Figure 1.- The influence of rivet pitch on the strength of a short sheet-stringer panel showing the three predominant modes of failure.

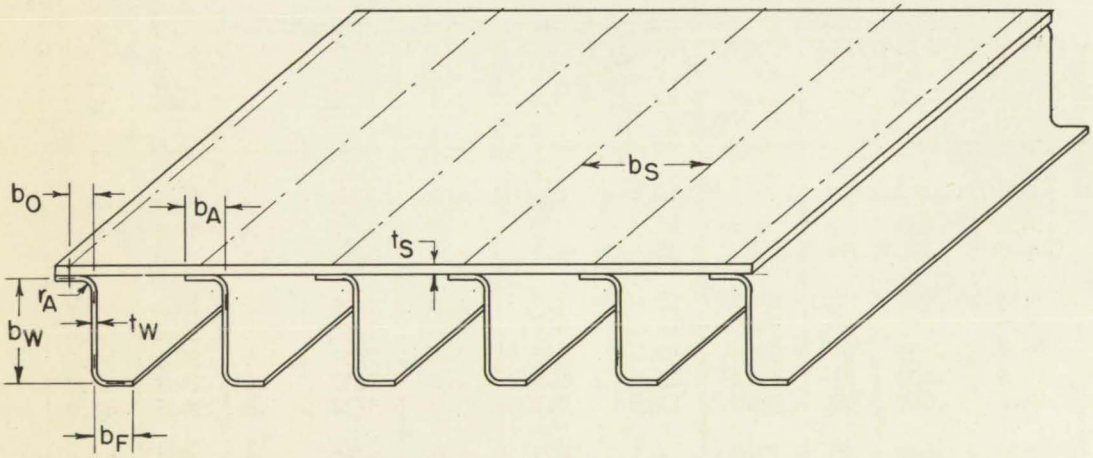

Figure 2.- A sheet-stringer panel.

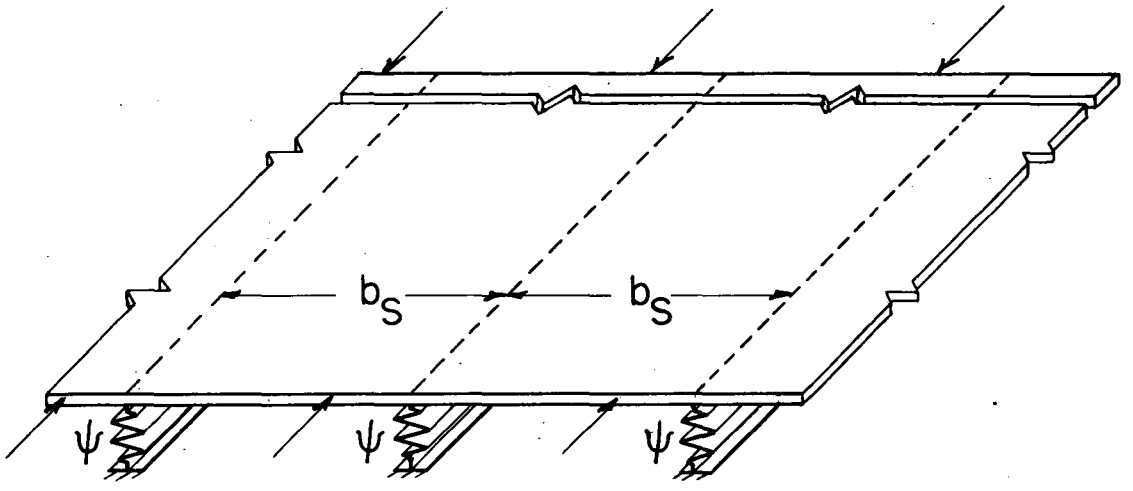

Figure 3.- Idealized structure used in analysis of sheet-stringer panel.

Figure 4.- Cross section of idealized structure at the crest of a buckle.

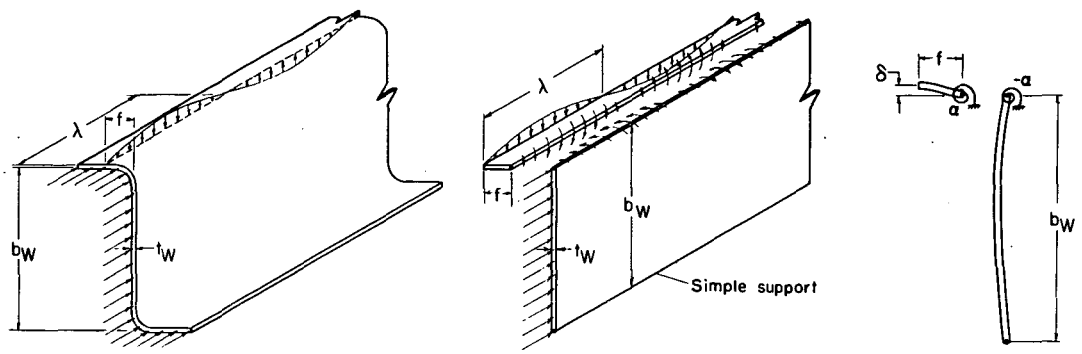

(a) Loads on stringer. (b) Idealized stringer. (c) Distortion of idealized stringer.

Figure 5.- Loads and deformations used in the calculation of the deflectional stiffness of short Z-section stringers.

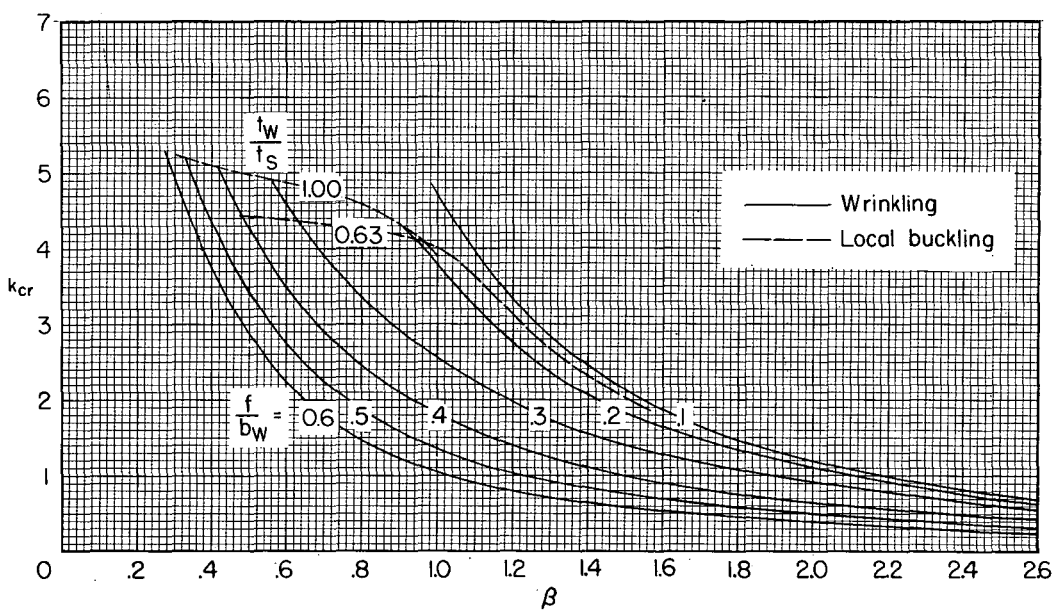

Figure 6.- The initial instability of Z-stiffened panels subjected to axial compressive loads. $\frac{\sigma_{cr}}{\eta} = \frac{k_{cr}\pi^2 E}{12(1-\mu^2)}\left(\frac{t_s}{b_s}\right)^2$.

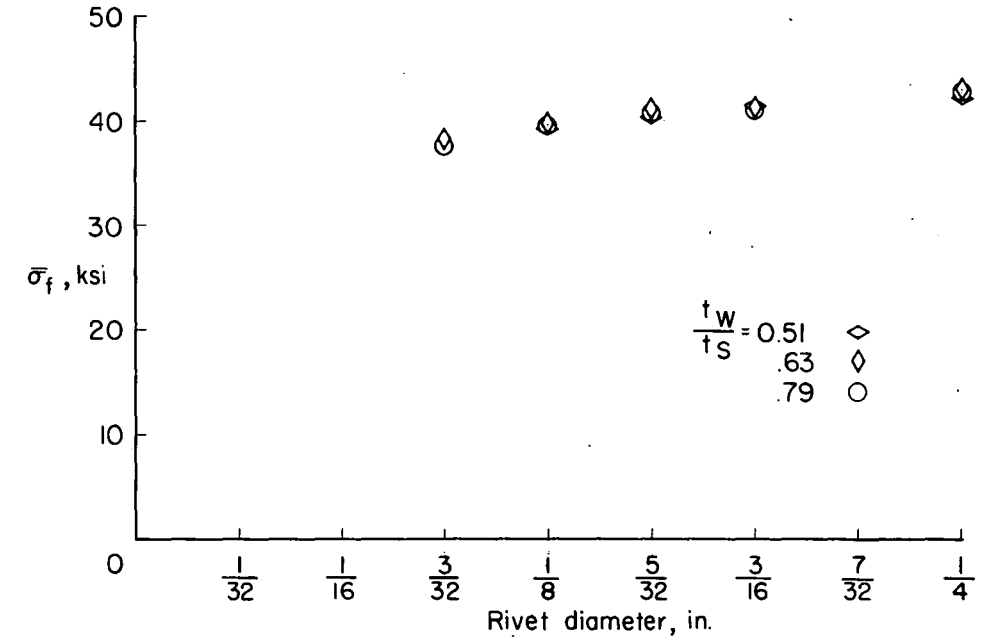

(a) Rivet pitch, 7/8 in.

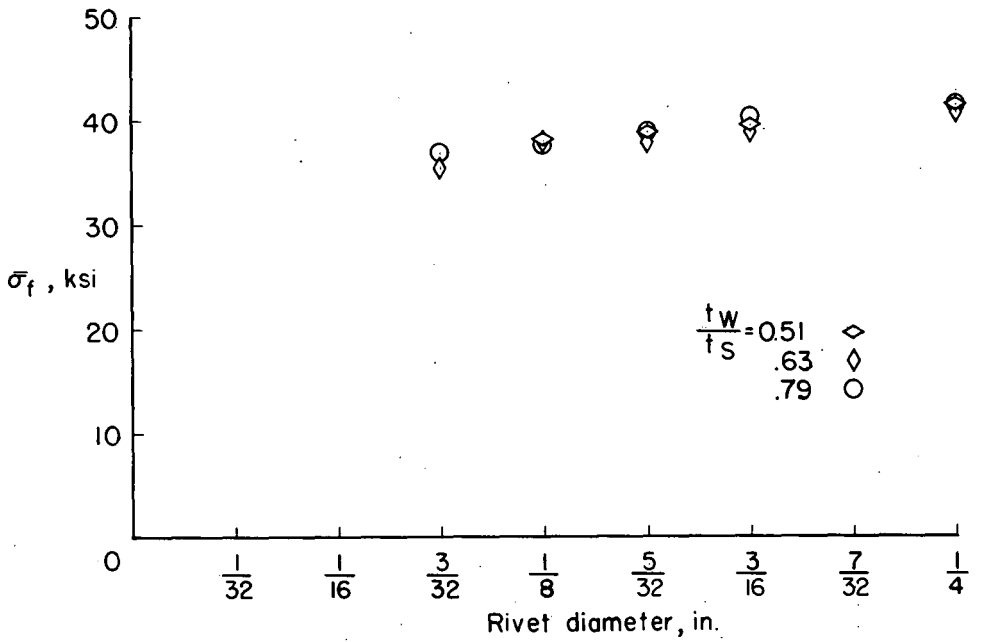

(b) Rivet pitch, $1\frac{7}{32}$ in.

Figure 7.- Comparison of average stress at maximum load for panels of reference 9 for three values of t_W/t_S. b_W/t_W = 20; b_S/t_S = 25; b_O/t_W = 5.6; t_W = 0.064 in.

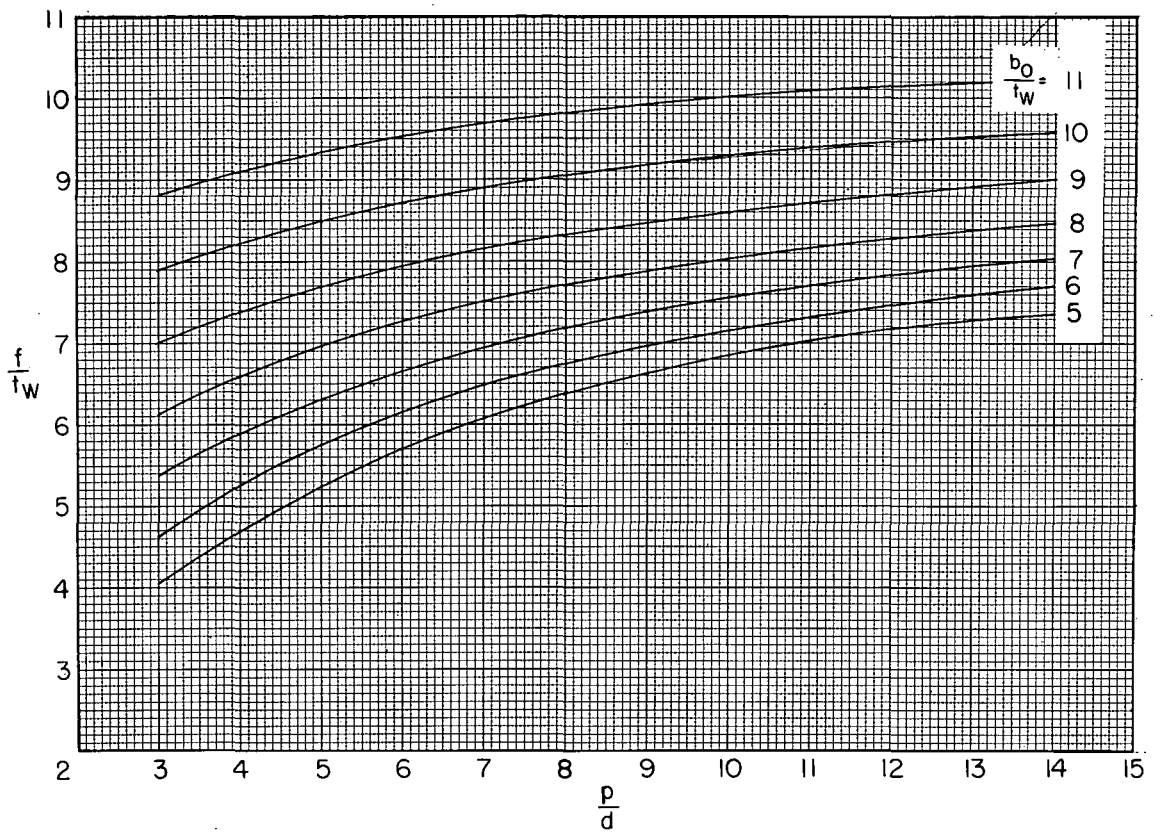

Figure 8.- Experimentally determined values of effective rivet offset for Z and channel stringers and full-depth channel webs.

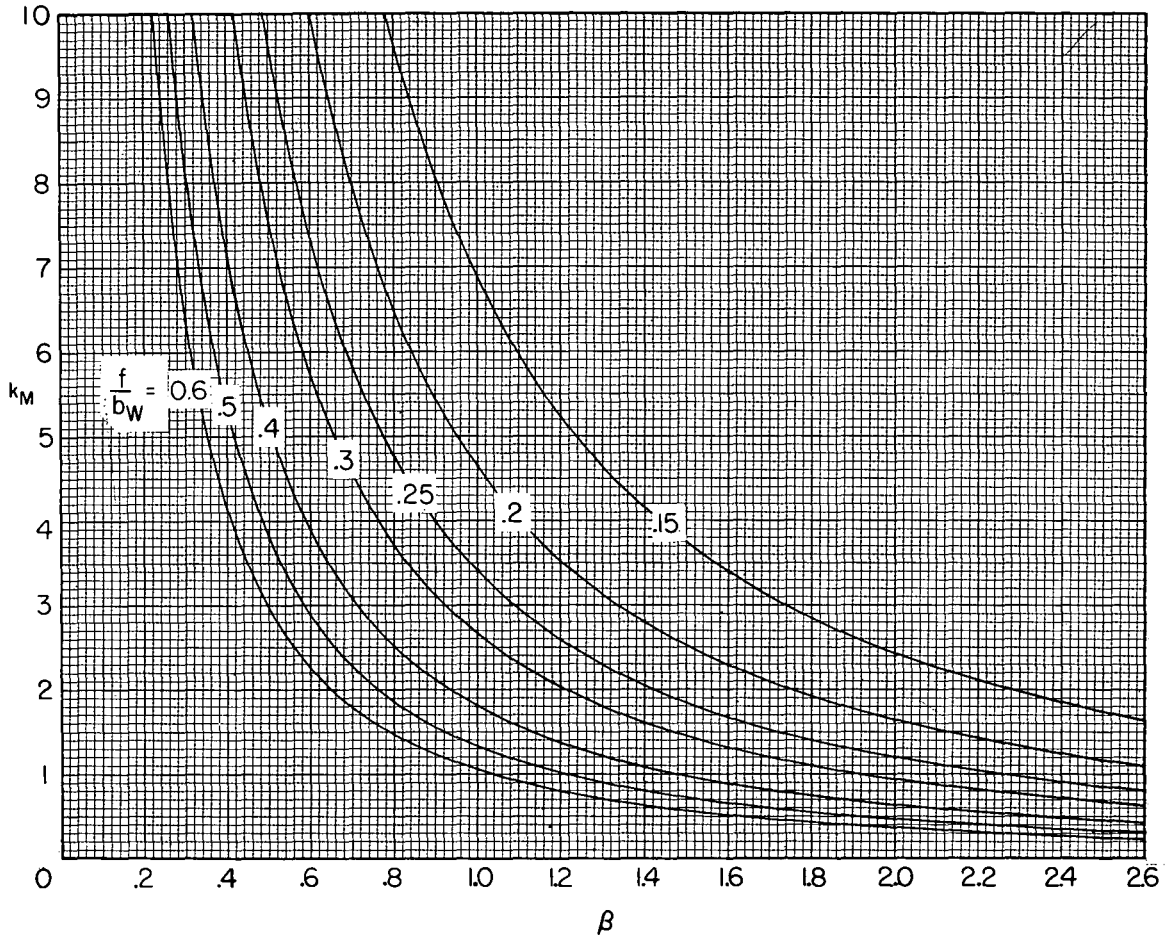

Figure 9.- Maximum stress coefficients for sheet-stringer panels that fail by wrinkling. $\frac{\sigma_M}{\eta} = \frac{k_M \pi^2 E}{12(1 - \mu^2)} \left(\frac{t_s}{b_s}\right)^2$.

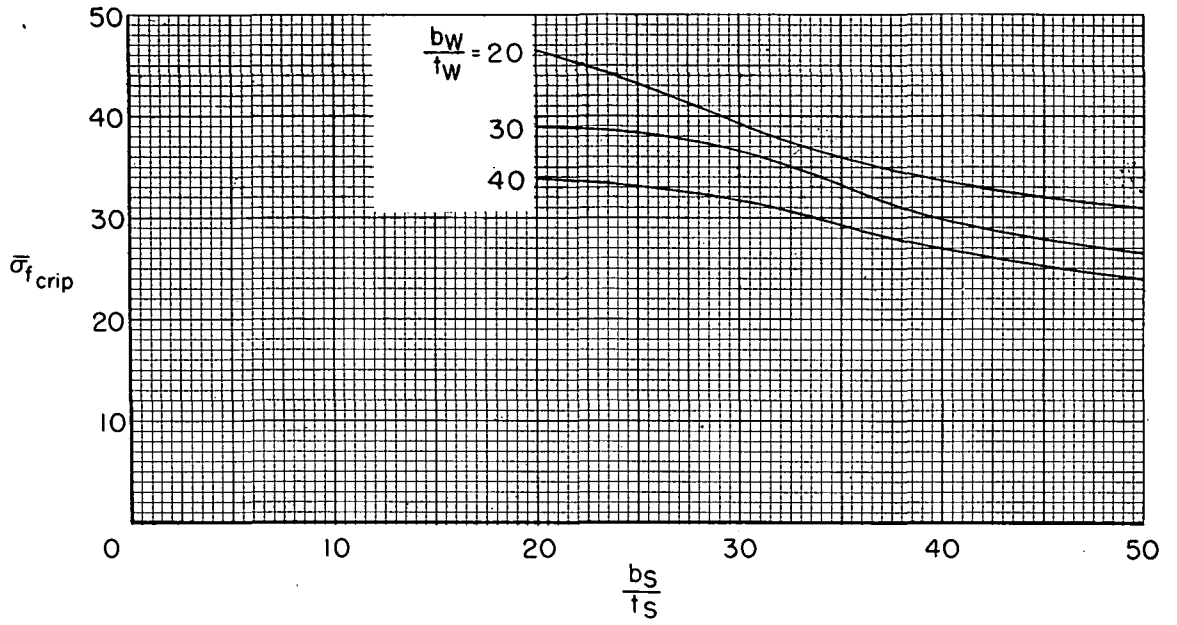

(a) $t_W/t_S = 0.63$.

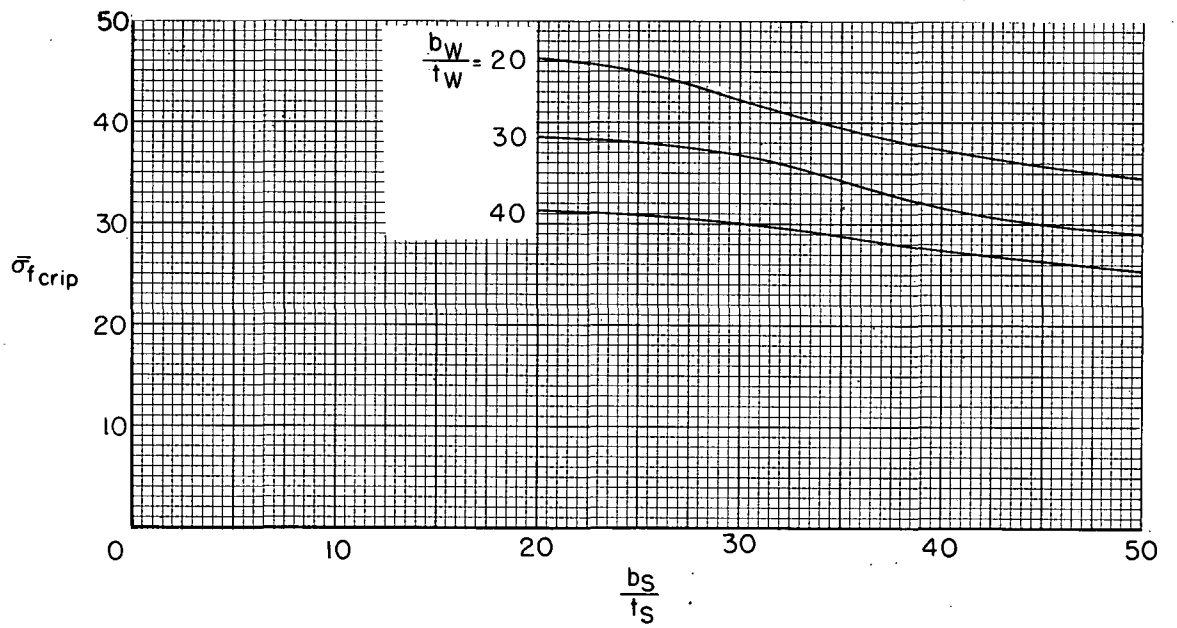

(b) $t_W/t_S = 1.00$.

Figure 10.- The strength of 2024-T3 aluminum-alloy Z-stiffened panels in the local mode. $b_F/b_W = 0.40$.

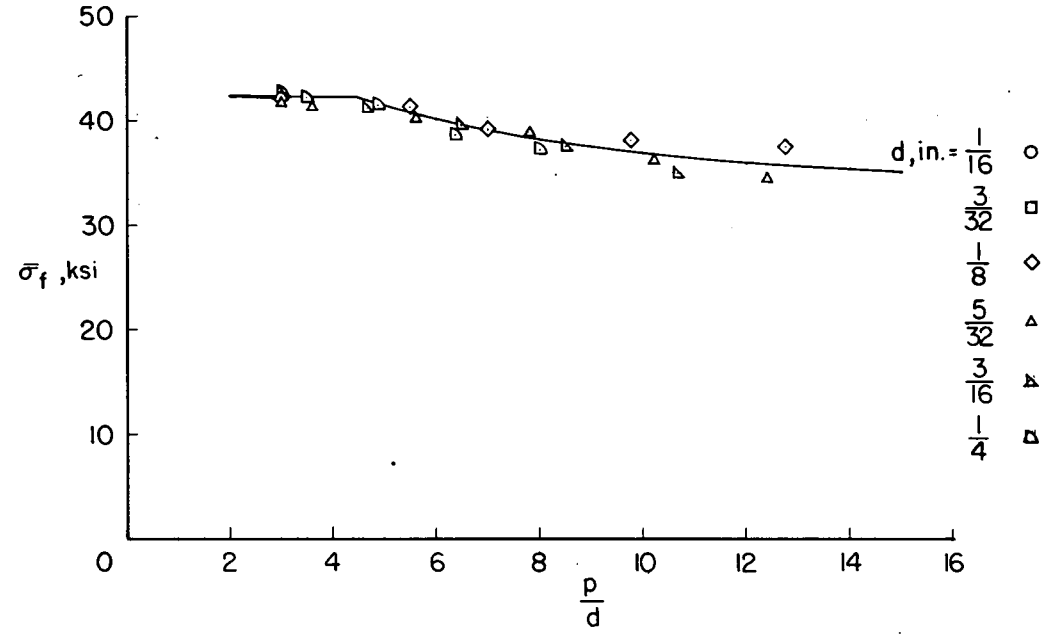

(a) $t_W/t_S = 0.51$.

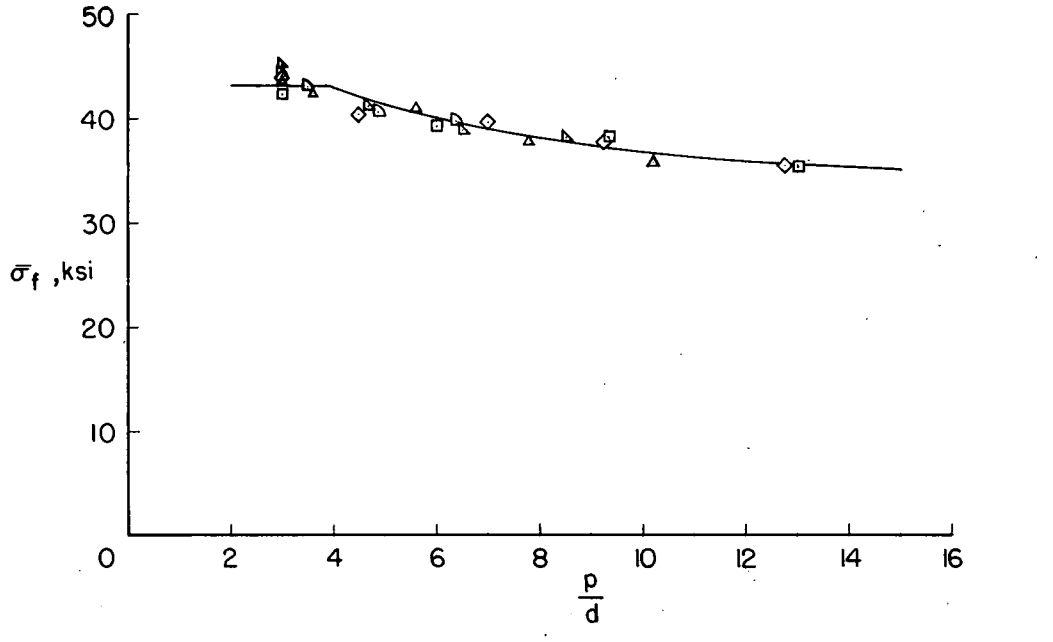

(b) $t_W/t_S = 0.63$.

Figure 11.- Comparison of calculated and experimental failing stresses of 2024-T3 Z-stiffened panels of reference 9 for five values of t_W/t_S. $b_W/t_W = 20$; $b_S/t_S = 25$; $b_O/t_W = 5.6$; $t_W = 0.064$ in.

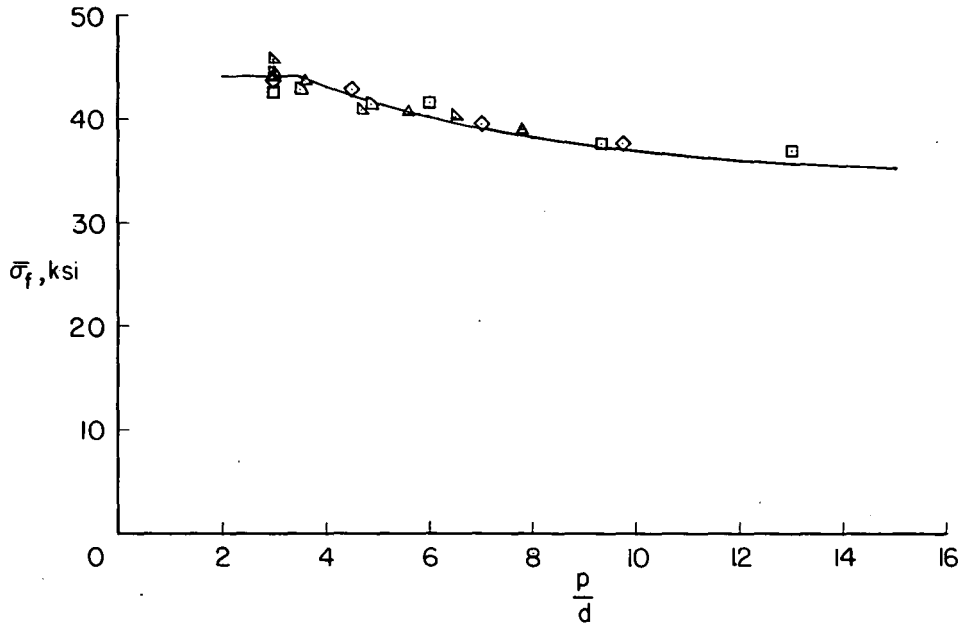

(c) $t_W/t_S = 0.79$.

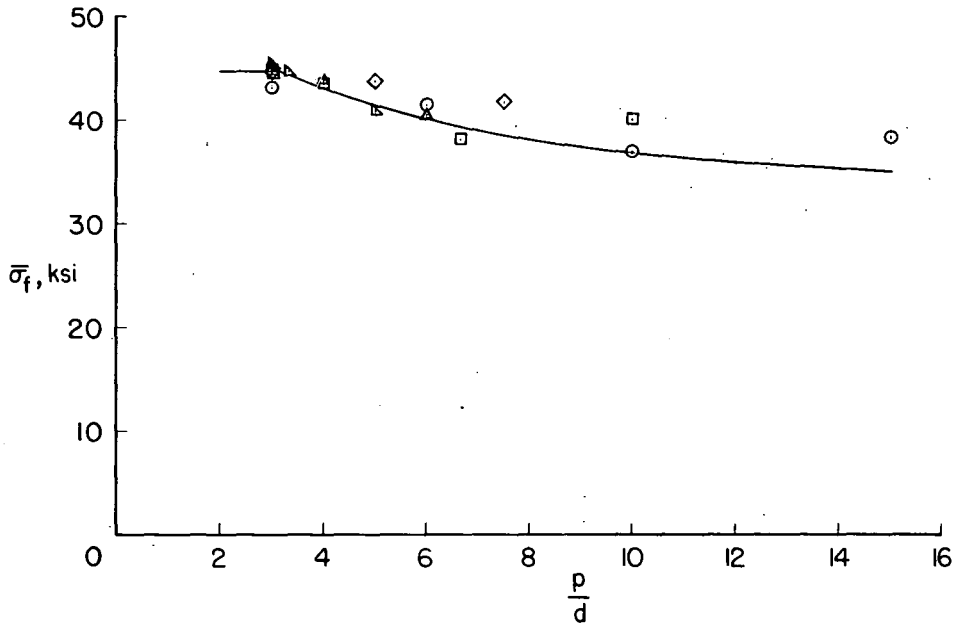

(d) $t_W/t_S = 1.00$.

Figure 11.- Continued.

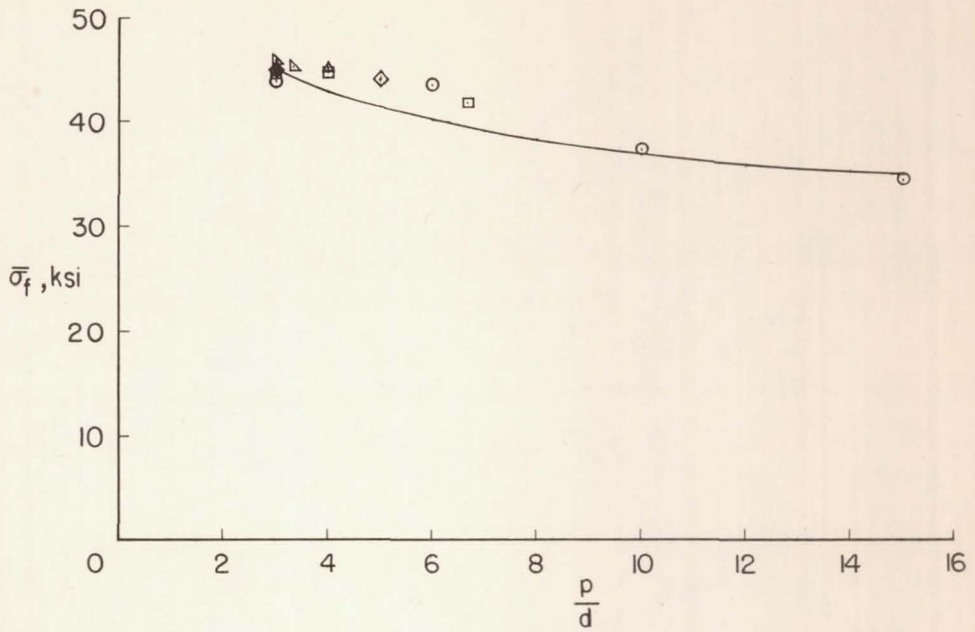

(e) $t_W/t_S = 1.25$.

Figure 11.- Concluded.

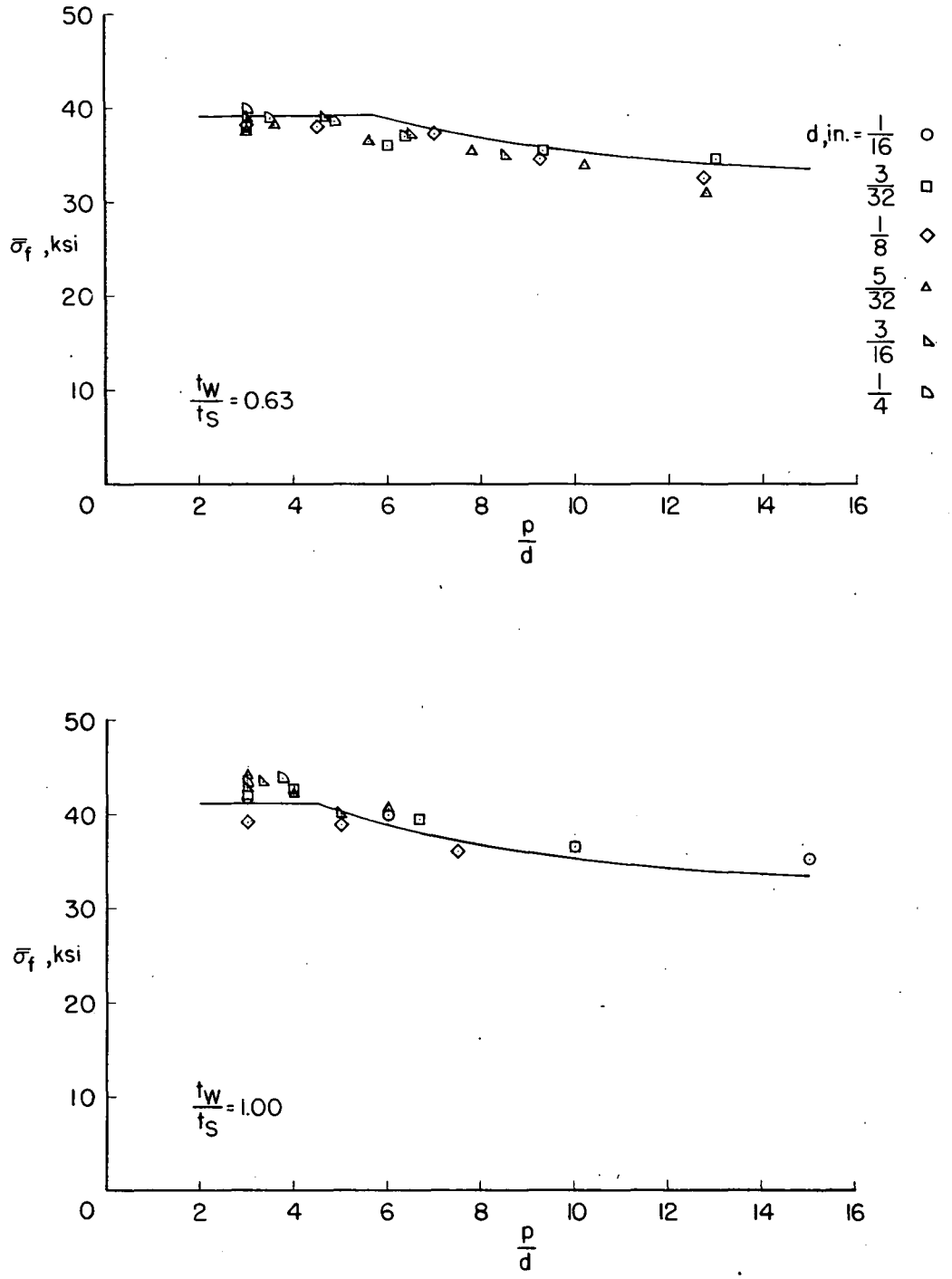

(a) $b_s/t_s = 30$.

Figure 12.- Comparison of calculated and experimental failing stresses of 2024-T3 Z-stiffened panels of reference 15 for four values of b_s/t_s at two values of t_w/t_s. $b_w/t_w = 20$; $b_o/t_w = 5.6$; $t_w = 0.064$ in.

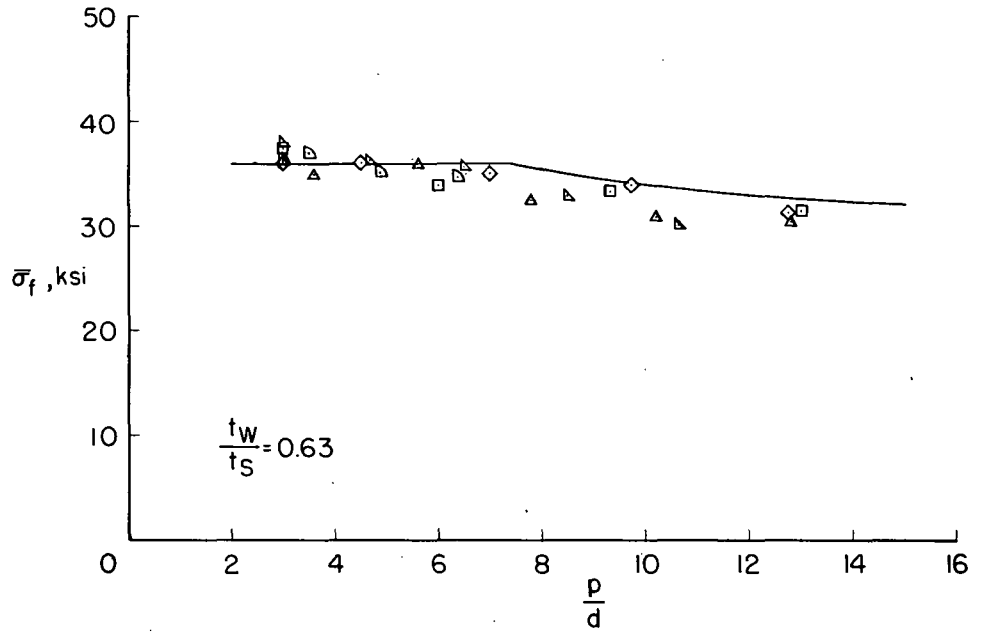

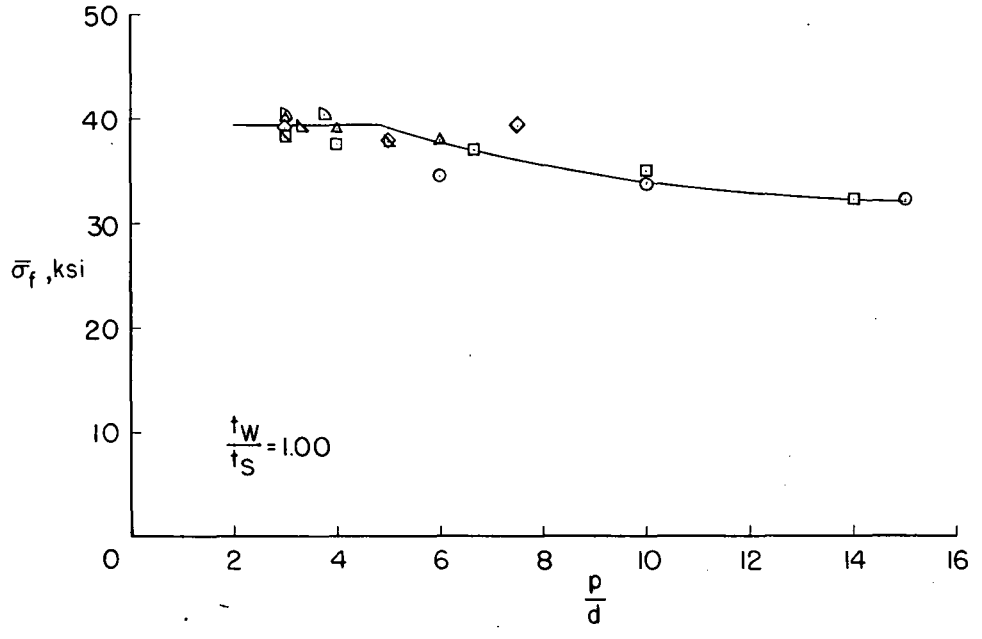

(b) $b_s/t_s = 35$.

Figure 12.- Continued.

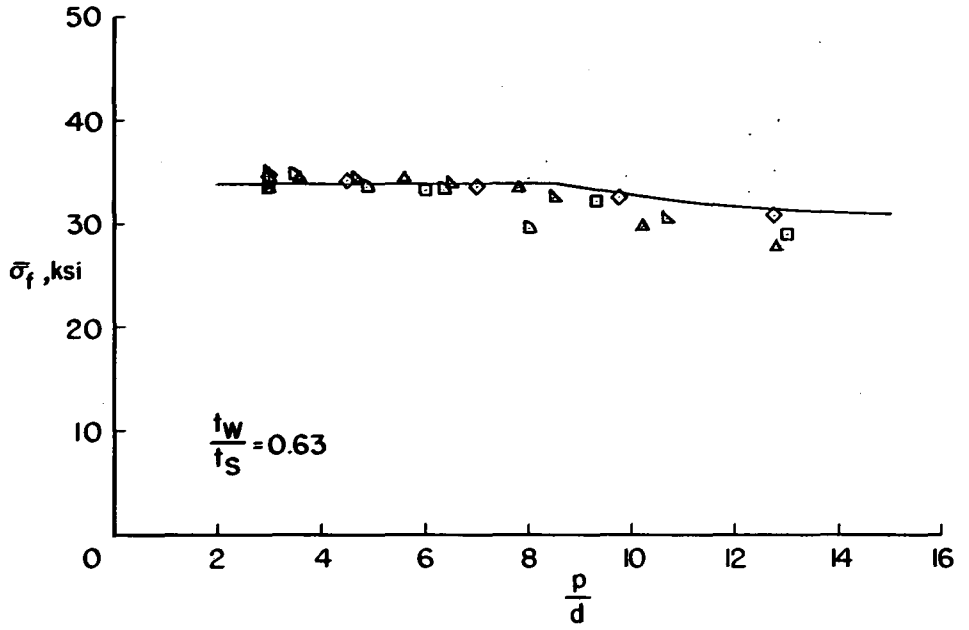

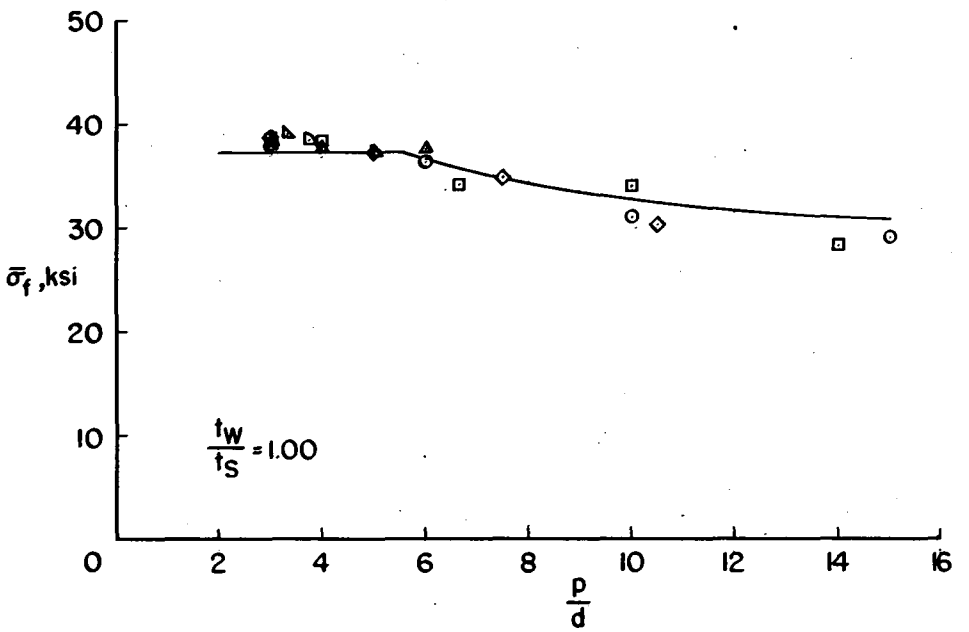

(c) $b_s/t_s = 40$.

Figure 12.- Continued.

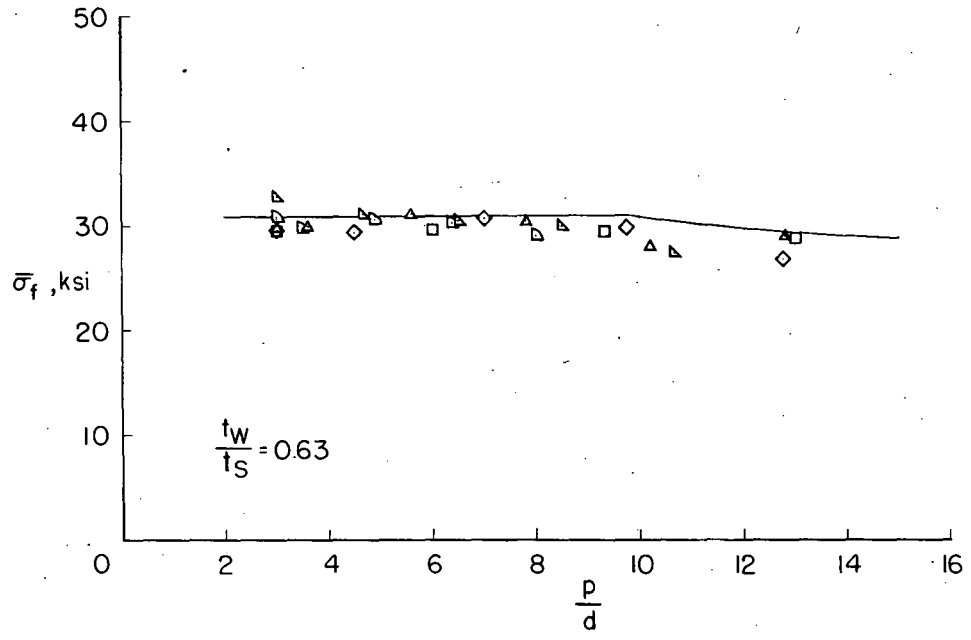

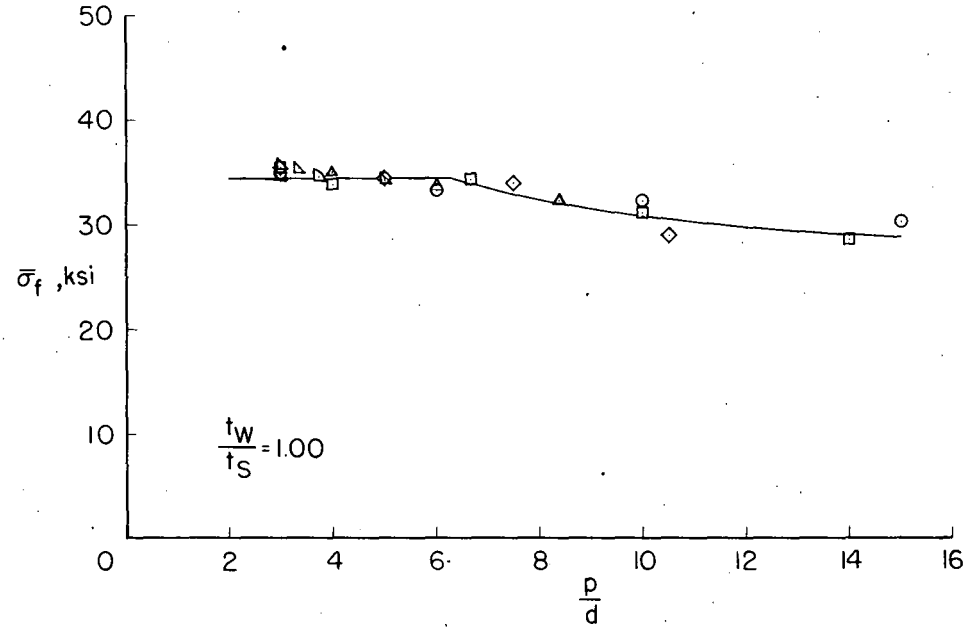

(d) $b_s/t_s = 50$.

Figure 12.- Concluded.

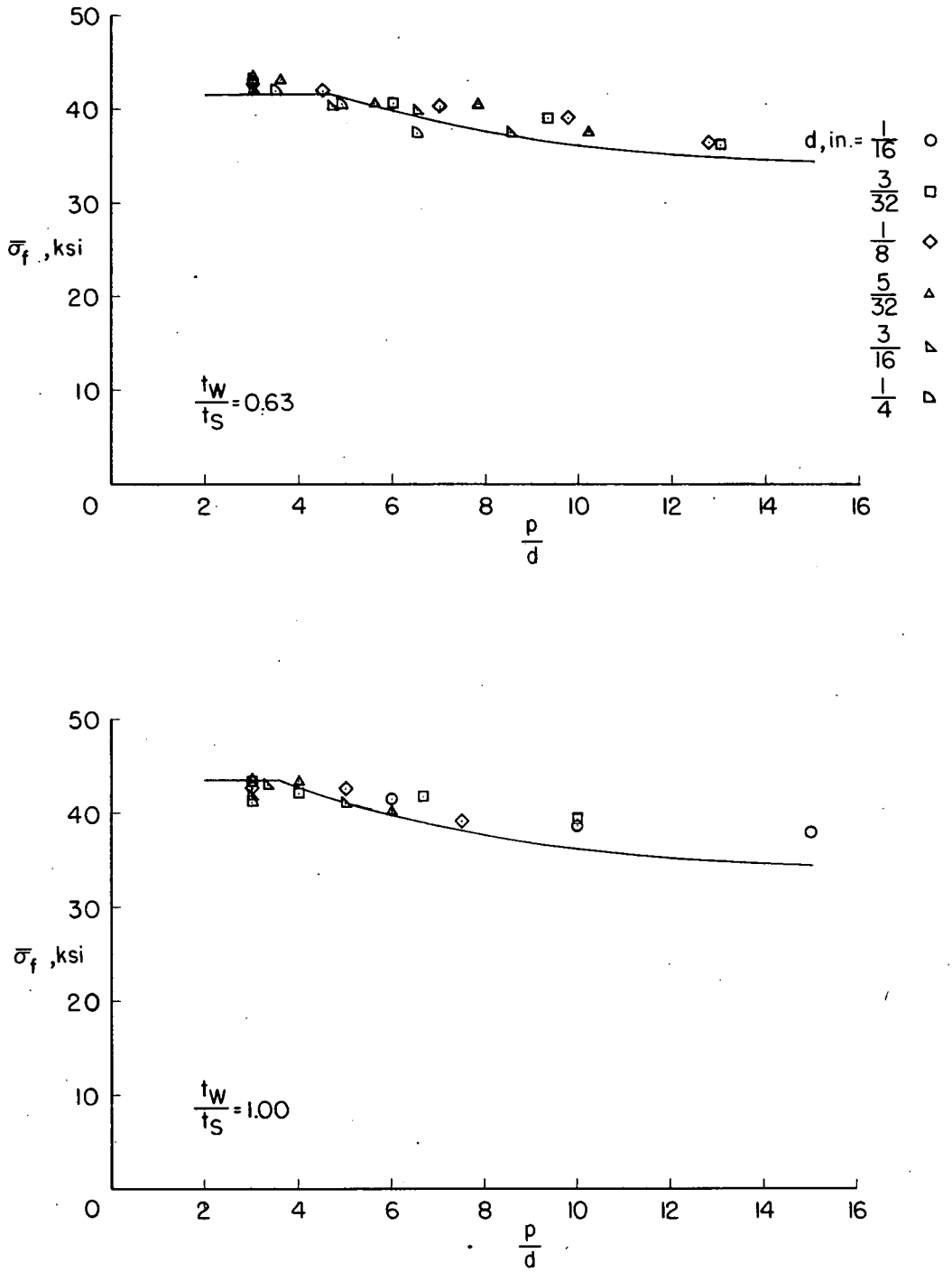

(a) $b_w/t_w = 25$.

Figure 13.- Comparison of calculated and experimental failing stresses of 2024-T3 Z-stiffened panels of reference 16 for four values of b_w/t_w and two values of t_w/t_s. $b_s/t_s = 25$; $b_o/t_w = 5.6$; $t_w = 0.064$ in.

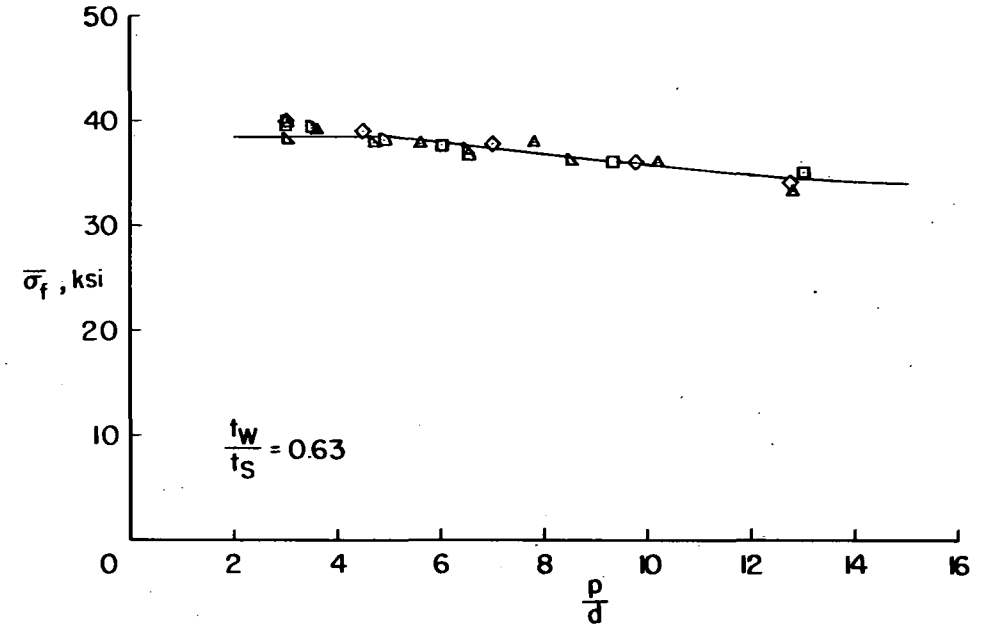

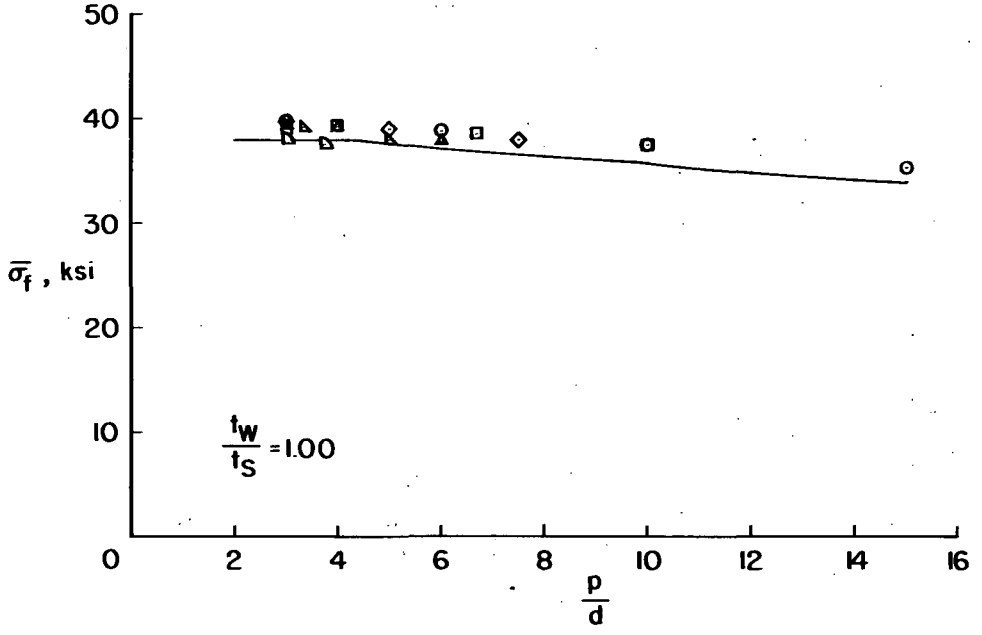

(b) $b_w/t_w = 30.$

Figure 13.- Continued.

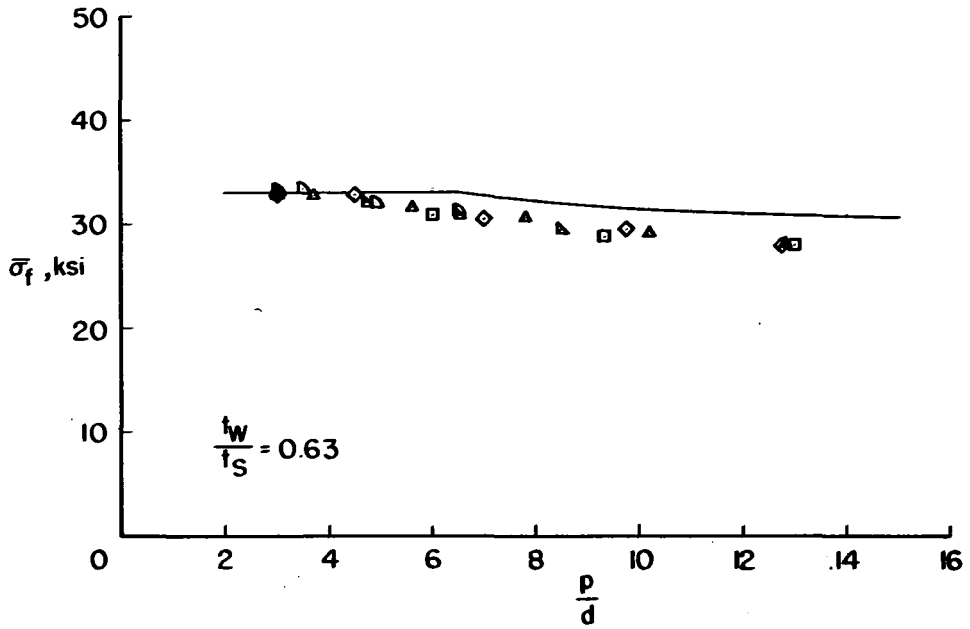

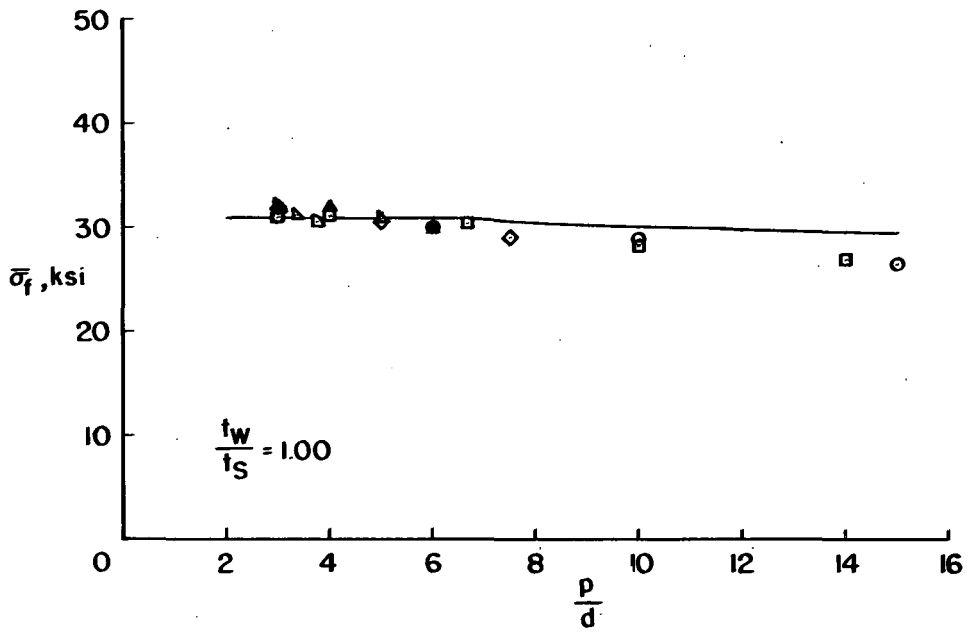

(c) $b_w/t_w = 40$.

Figure 13.- Continued.

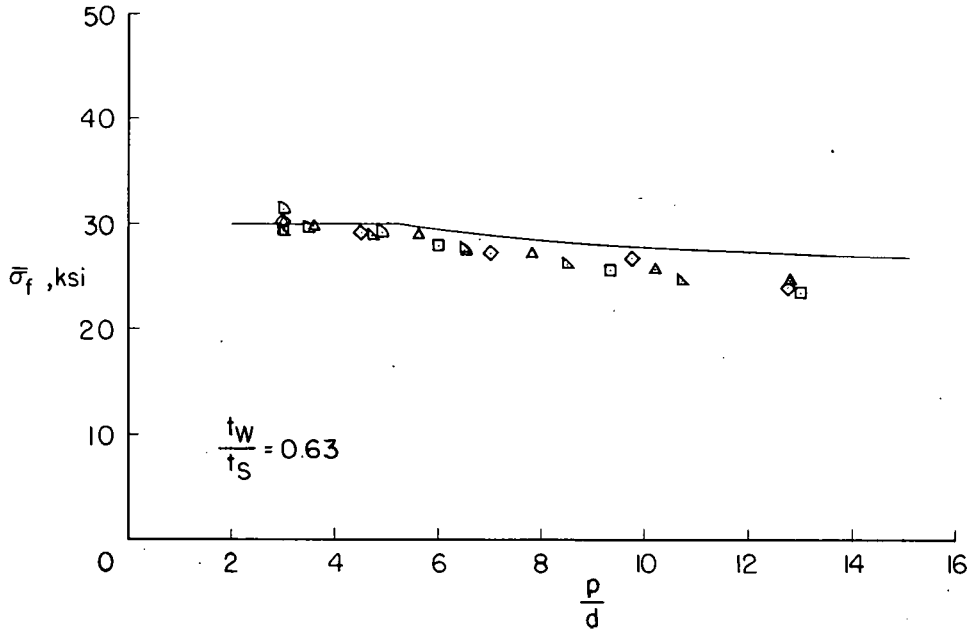

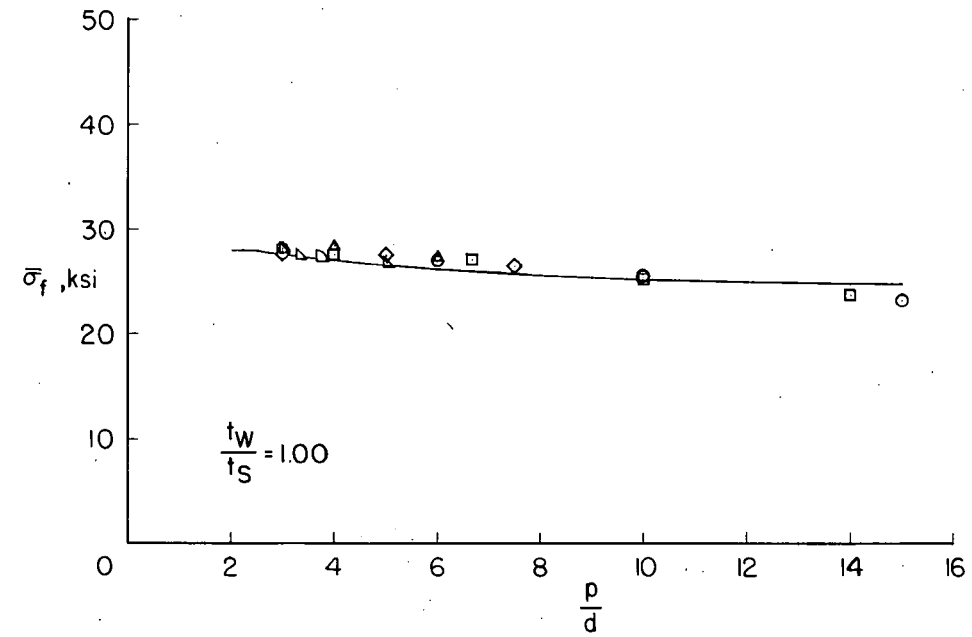

(d) $b_w/t_w = 50$.

Figure 13.- Concluded.

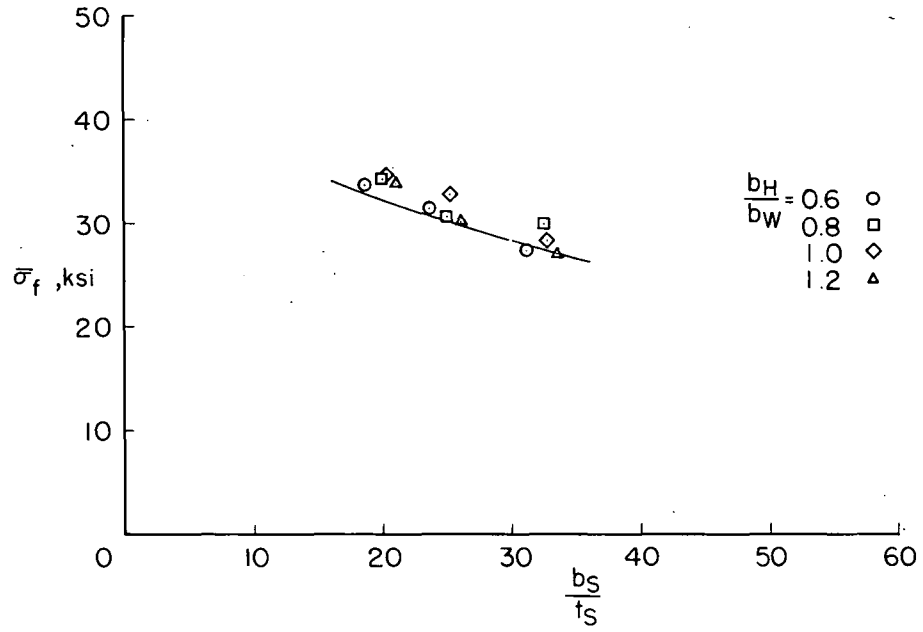

(a) $b_W/t_W = 19.$

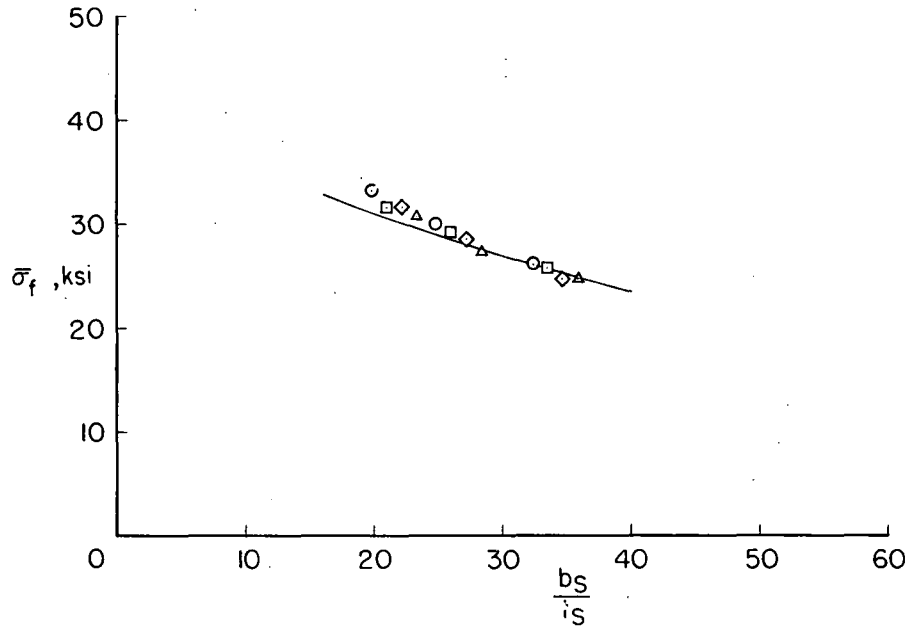

(b) $b_W/t_W = 29.$

Figure 14.- Comparison of calculated and experimental failing stresses of 2024-T3 hat-stiffened panels of reference 25 for three values of b_W/t_W and four values of b_H/b_W. $t_W/t_S = 0.39$; $p/d = 16/3$; $b_O/t_W = 11.0$; $t_W = 0.040$ in.

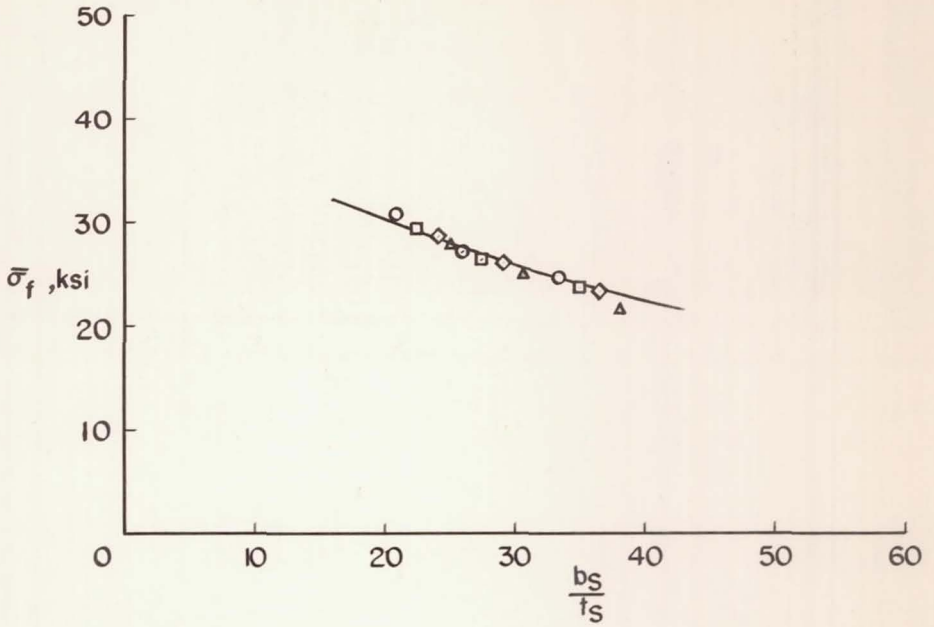

(c) $b_w/t_w = 39.$

Figure 14.- Concluded.

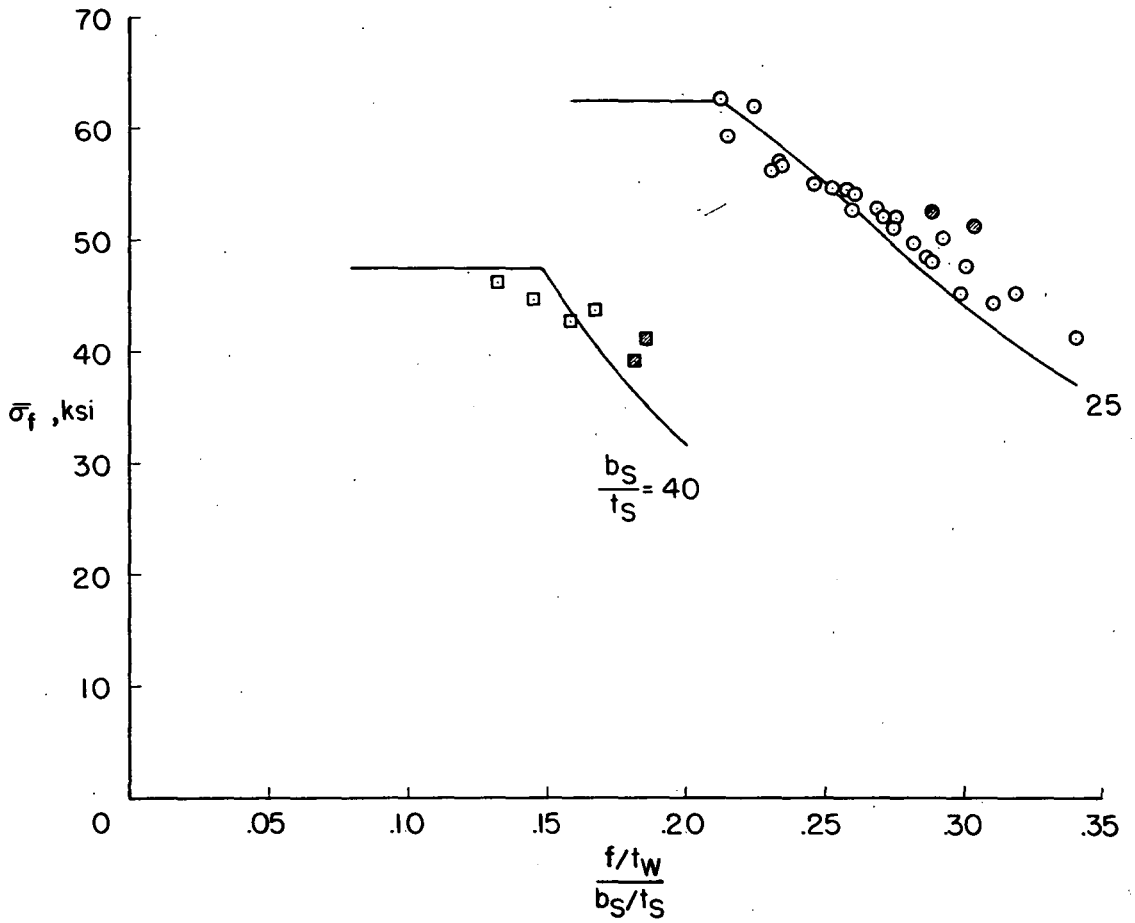

Figure 15.- Comparison of calculated and experimental failing stresses of 7075-T6 Z-stiffened panels of table I. The shaded points represent panels which had stringers with $r_A/t_W = 6.0$.

NACA-Langley - 3-29-55 - 1000